The Thesis Committee for Anish Satish Dabhi
Certifies that this is the approved version of the following thesis:

Biodegradable Natural Fiber Composites: Fabrication and Characterization of Hemp Fiber with PLA Powder Composites

APPROVED BY

SUPERVISING COMMITTEE:

Wei Li, Supervisor

Jonathan Y. Chen

Biodegradable Natural Fiber Composites: Fabrication and Characterization of Hemp Fiber with PLA Powder Composites

by

Anish Satish Dabhi, B.E., M.S.

Thesis

Presented to the Faculty of the Graduate School of

The University of Texas at Austin

in Partial Fulfillment

of the Requirements

for the Degree of

Master of Science in Engineering

The University of Texas at Austin

May 2016

Acknowledgements

I would like to first and foremost thank my advisor, supervisor and mentor, Dr. Wei Li, for his continuous support and motivation. His encouragement and enthusiasm continually helped to guide the research, and I am sincerely grateful for his guidance. He has and will continue to be an inspiration in my work.

I would also like to thank Dr. Jonathan Chen, my reader of the thesis for his assistance and inputs throughout the project. His help truly contributed to conducting the research.

Finally I would like to thank all the members of the Nano and Bio-Material Processing and Manufacturing Lab – Russel Bourduin, Wei Jiang, Hao Xin, Xiaoran Li, Jungyu Ock, Daniel Justiss and also Yue Liu for their invaluable assistance, productive discussions and companionship throughout the course of the degree work.

Abstract

Biodegradable Natural Fiber Composites: Fabrication and Characterization of Hemp Fiber with PLA Powder Composites

Anish Satish Dabhi, M.S.E.

The University of Texas at Austin, 2016

Supervisor: Wei Li

Interest in natural fiber composites has been increasing in recent years due to their environmental benefits, along with weight reduction and economic viability. The composites in some cases have proven to exceed glass fiber composites and are suitable substitutes for the same. Hemp-Polylactic acid (PLA) composites were fabricated using a novel method, wherein PLA powder is mixed with hemp fibers through a needle punching process. The composites were produced at three different fiber loading levels of 35%, 50% and 55% and showed differently finished top and bottom surfaces, the top being plastic and the bottom being fibrous. The mechanical, acoustic and thermal properties were characterized and it was found that 50% composites provided the best results. Overall, the composites performed in the range of previously documented non modified natural fiber composites, giving the fabrication process validity.

The tensile and impact tests showed acceptable strengths and also demonstrated low shattering probability due to fiber entanglement. This was also seen from the high values of elongation at break. Dynamic mechanical analysis (DMA) showed the highest storage modulus for

the 50% fiber loaded samples and an increased glass transition temperature compared to neat PLA. The samples showed low thermal conductivity values, comparable to asbestos, showing good thermal insulation properties. Acoustic absorption coefficients were measured using a two microphone impedance test at varying high and low frequencies. The coefficients showed high acoustic absorption even at moderate frequency levels, owing to the dampening effect of the hemp fibers.

Table of Contents

List of Tables

List of Figures

Chapter 1 Introduction

1.1 Motivation of Research

With the current growing awareness and concern about the environment and sustainability, the academic and industrial sectors have started to lean towards greener technologies, a major part of which is played by material development. Legislative End-of-Life of Vehicles (ELV) recycling systems have been established in the European Union (EU), Japan, Korea, and China, while in the US, ELV recycling is managed under existing laws on environmental protection [1]. The European Commission had proposed a European Guideline 2000/53/EC that set a goal of improving automotive reuse and recycling, wherein 80% of a vehicle by weight must be recyclable by 2005. This recyclable percentage was increased to 85% by 2015 [2]. Data shows that by 2013 the EU had reached 85.3% total reuse and recyclability of vehicles, which increased from 78.4% in 2005 [3]. In modern passenger cars, plastics constitute about 50% by volume and 10% by weight of the vehicle, making recyclability of these parts is essential. For this and other such purposes agricultural plants, forestry products and biological materials have been in the limelight of research. Plant materials, particularly with fibrous stalks, are among the most widely researched avenues. Plant fibers are made of cellulose fibrils, which have unique properties, based on the plant composition and structural hierarchy. Due to these properties, they prove to be valuable replacements for glass and carbon fibers as fillers in composites [4]. When used to make polymer composites, they provide enhanced characteristics of mechanical strength, sound absorption and dampening, vibration reduction, heat resistance, weight reduction, non-abrasiveness to equipment, non-hazardous nature, less energy consumption, recyclability, and

ecological stability. Examples of such plants include hemp, flax, kenaf, jute, and ramie. These plants have been specified because of their availability and renewability, biodegradability, cost effectiveness, low density, and exceptional specific characteristics as opposed to synthetic fillers [4].

Natural fiber reinforced polymer composites have been tested and developed using the above mentioned plant fibers along with thermoplastic polymers such as polypropylene (PP), polyethylene and poly-vinyl chloride (PVC), and with thermosetting polymers such as epoxy, phenolic and polyester resins [4]. These materials are suitable for application in automotive and aerospace industries, sports, construction, and packaging [5].

Figure 1-1 Automobile components made of natural fibers. Source: globalhemp.com

The most common and scalable methods to manufacture natural fiber composites (NFCs) are injection molding and compression molding, depending on the type of fiber used. Resin transfer molding, pultrusion, vacuum bagging and hand lay-up methods are also used [6]. When manufactured using compression molding, first a composite fiber mat is made. This is typically

done by mixing polymer fibers and natural fibers in the desired ratio and subjecting to a carding process. Subsequently, the mat is needle punched to form a natural fiber reinforced non-woven felt. This felt is then compression molded to form the final composite material.

This process requires the polymer material to be formed into fibers through a spinning process. Various methods of spinning used industrially are – wet, dry, dry jet-wet, melt, gel, and electrospinning [7]. This step in the manufacturing process consumes energy, uses chemical solvents in some cases, and adds to the material cost. The method proposed in this research utilizes the polymer in its powder form to be incorporated into the non-woven natural fiber felt, eliminating the step of polymer fiber spinning and hence streamlining the composite manufacturing process.

1.2 Research Objectives

The goal of this research is to manufacture and characterize non-woven hemp-PLA composites using a unique method and to determine the effectiveness of this method, through experimental studies. The following objectives have been identified:

1. To develop a fabrication method for composite manufacture utilizing a non-woven hemp fiber mat and PLA powder.
2. To characterize the composite material by conducting tests, including tensile strength, impact strength, dynamic mechanical analysis, thermal conductivity, and acoustic absorption.
3. To analyze and compare the characteristics to previously documented results for natural fiber composites.

1.3 Organization of Thesis

The thesis is divided into five chapters. Chapter 1 is the introduction and motivation behind the work. Chapter 2 gives the necessary background on natural fibers, hemp, PLA, and non-woven natural fiber composites. Previous work by researchers is cited here with their results for comparison. Chapter 3 describes the experimentation process, including the materials and equipment used. The process is divided into 3 phases – (i) felt fabrication, (ii) compression molding, and (iii) final sample preparation and characterization. The first two phases provide input for the final sample fabrication process, phase (iii). Chapter 4 is a discussion of the results from the experimentation. The mechanical properties are characterized and compared to existing reports. Finally, Chapter 5 concludes the thesis with a summary and recommendations for future work.

Appendices are cited throughout the thesis and are attached at the end.

Chapter 2 Literature Review

2.1 Natural Fibers

Natural fibers can refer to fibers from any natural source – plant, animal or mineral. Mineral fibers include asbestos, ceramic and metal fibers which are not biodegradable and are energy intensive. Animal fibers consist largely of protein [8] and include silk, hair, wool, fur, feathers, etc. Plant fibers, particularly bast fibers, are made primarily of cellulose, lignin and hemicellulose, which give them their unique properties [9]. They are referred to as lignocellulosic fibers. The most widely used plant fibers for the purpose of composite polymers are hemp, kenaf, jute, ramie and flax [4].

2.1.1. Composition of Lignocellulosic Fibers

Cellulose is the most abundant organic compound on earth. The cellulose molecule is a polysaccharide made of 10,000- 25,000 glucose monomers with a 1-4 glycosidic linkage [10]. The presence of many hydroxyl groups along the cellulose chain results in the formation of a

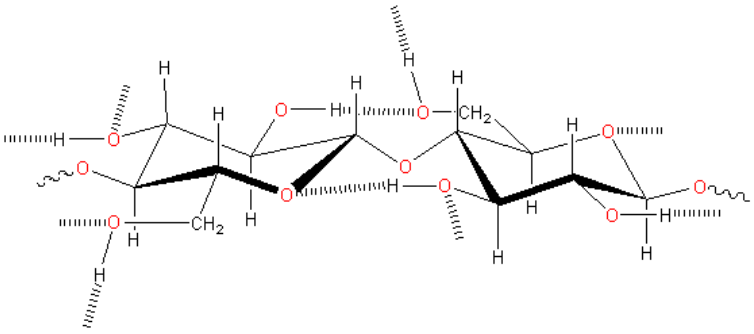

Figure 2-1 Structure of cellulose - Hydrogen bonding [10]

network of inter- and intramolecular hydrogen bonds (Figure 2-1). This ordered molecular arrangement is the basis of a crystal structure called microfibrils [11]. Microfibrils have widths, lengths, shapes and crystallinities that may vary depending on the origin of cellulose. Widths can range from 2-3 nm for the cell wall of primary tissues of some plants to over 60 nm for certain algae [12]. Microfibrils are surrounded by hemicelluloses and lignin, which bind many of these microfibrils together to form a fibril- matrix structure, which form the building units of the cell wall (Figure 2-2). The cell wall has a tubular structure to necessitate the flow of water and nutrients. These microscopic tubes make up the fibrous material of the plant stalk [13].

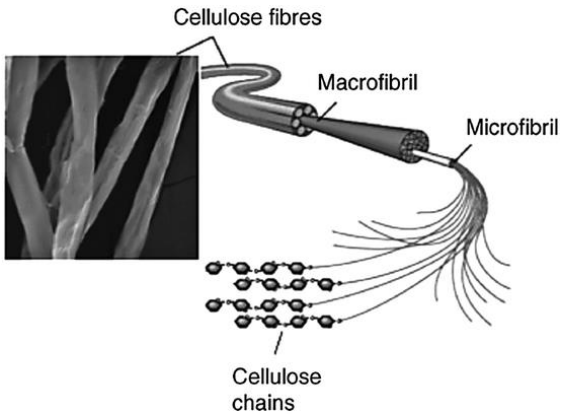

Figure 2-2 Hierarchical structure of cellulose fiber [11]

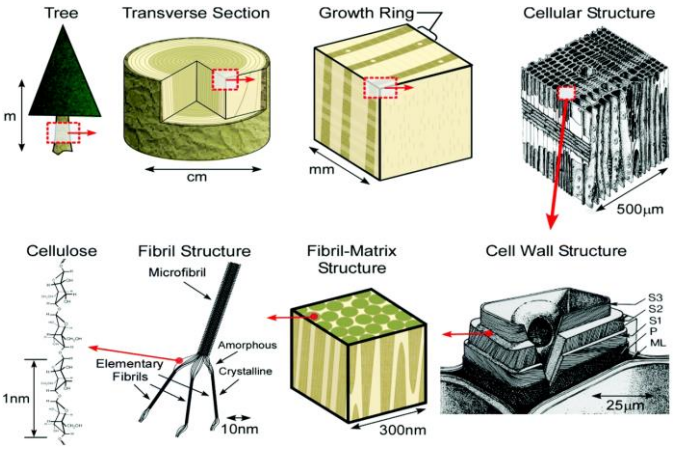

Figure 2-3 Scale of hierarchical structure [13]

2.1.2 Characteristics of Plant Fibers

Owing to the hierarchical structure of plant fibers, each has its unique properties, advantages and disadvantages. A common trait amongst the plant fibers is low density and hence high specific characteristics, as can be seen in Table 2-1.

Natural fibers have a few disadvantages, which can also be attributed to their unique cellulosic structure. Moisture absorption is high for natural fibers (Table 2-1), which is primarily due to the availability of hydroxide groups on the surface of the lignocellulosic fibers [14]. These reactive sites form hydrogen bonds with water and the tubular or hollow nature of the fibers allows the water to be trapped. Presence of moisture in the composite material distorts its mechanical characteristics [14]. However, the highly reactive OH sites can also be used to their advantage by introducing compounds to modify the surface properties of the fibers. Pickering (2007) modified hemp fibers with 10% (wt.) NaOH solution to produce strong fibers with low lignin content and good fiber separation [15]. Dai (2012) used two-step nanocellulose modification of hemp fibers and investigated the mechanisms of the efficacy of the modification. The results showed that the nano-modification significantly increased the mechanical and interfacial properties of hemp fibers. The optimized condition (pH 11, 0.1% DTAB) of the nano-modification resulted in an

Table 2-1 Properties and comparison of natural fibers with glass fiber [14]

Properties	Fibre								
	E-glass	flax	hemp	jute	ramie	coir	sisal	abaca	cotton
Density g/cm^3	2.55	1.4	1.48	1.46	1.5	1.25	1.33	1.5	1.51
Tensile strength* 10E^6 N/m^2	2400	800 - 1500	550 - 900	400 - 800	500	220	600- 700	980	400
E-modulus (GPa)	73	60 - 80	70	10 - 30	44	6	38		12
Specific (E/density)	29	26 - 46	47	7 - 21	29	5	29		8
Elongation at failure (%)	3	1.2 - 1.6	1.6	1.8	2	15 - 25	2 - 3		3 - 10
Moisture absorption (%)	-	7	8	12	12 -17	10	11		8 - 25
price/Kg ($), raw (mat/fabric)	1.3 (1.7/3.8)	- 1.5 (2/4)	0.6 - 1.8 (2/4)	0.35 1.5/0.9 - 2	1.5 - 2.5	0.25 -0.5	0.6 - 0.7	1.5 - 2.5	1.5 - 2.2

increase of the modulus, tensile stress and tensile strain of hemp fibers by 36.13%, 72.80%, and 67.69%, respectively [16].

Since natural fibers are heterogeneous mixtures of organic materials, heat treatment at elevated temperatures can result in a variety of physical and chemical changes [17]. The thermal degradation temperature for natural fibers is considerably lower than synthetics fibers, which restricts working conditions. It has been shown [18] that thermal degradation of natural fibers generally occurs in two stages: one at 220–280°C temperature range and the other at 280–300°C range. The first range is associated with degradation of hemicellulose, whereas the second range is associated with degradation of cellulose and lignin. For most natural fibers decomposition reaches approximately 60% at around 215-310˚C [19]. Thermogravimetric analysis (TGA) of jute fibers shows that they start degrading at 240°C [20]. For flax fibers, it has been shown [21] that degradation starts at just above 160°C. Sridhar et al. [22] reported 60% reduction in tensile strength of jute fibers heated under vacuum at 300°C for two hours. Gonzalez and Myers [23] reported deterioration in mechanical properties of wood flour exposed to temperature range of 220 to 260°C for up to 68 hours.

2.2 Hemp Fibers

Hemp is a low cannabinoid (0-0.3% THC) variety of Cannabis Sativa, known commonly as Industrial Hemp. It has a history of use in construction, composites, making ropes and twine, paper and textiles dating back to ancient India and China [24]. It has re-gained popularity for use in composites in recent times for its remarkable mechanical properties and positive environmental impact. Acreage in hemp cultivation worldwide had been reported at about 200,000 acres globally in 2011 [25].

2.2.1. Properties

Hemp stalk is made up of nearly 75% cellulose (Table 2-2) [26]. It has a hollow tubular structure with a woody inner core, called hurd or shive, and long, tough outer bast fibers. They are glued

Table 2-2 Composition of hemp stalk [26]

	Cellulose	Pectin	Hemicelluloses	Lignin	Waxes and oils
wt.%	70.2-76.12	0.9-1.55	12.28-22.4	3.7-5.7	0.8-1.59

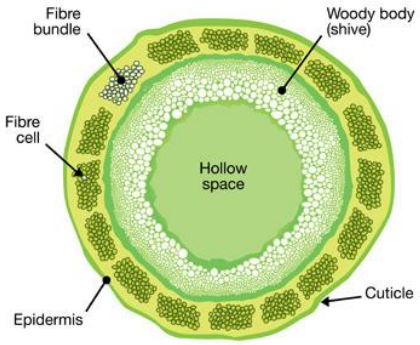

Figure 2-4 Hemp stalk cross-section [26]

together by lignin and hemicelluloses, and trace amounts of pectin. Figure 2-4 gives an idea of the cross-section of a single hemp stalk.

The tensile properties of hemp fiber have been studied and documented with varying results. Shahzad (2013) observed the dependence of tensile strength to the fiber width. The mean width of the fibers (circular dimension) was calculated to be 67 ± 26 μm (Figure 2-5). The tensile strength was evaluated at 277 ± 191 MPa, tensile modulus at 9.5 ± 5.8 GPa, and strain to failure at 2.3 ± 0.8% [17]. Prasad and Sain [27] reported fiber diameter of 66 μm and 250 MPa and 11 GPa for tensile strength and tensile modulus, respectively. Suardana et al. (2011) tested the tensile strengths of untreated hemp fibers as well as sodium hydroxide and silane treated hemp fibers (Table 2-3). They recorded a higher tensile strength of 962.5 MPa [28]. Fan et al. (2013) documented the tensile strengths of unmodified hemp along with DTAB modified and nanocellulose modified hemp fiber (Table 2-4). Unmodified hemp fiber was shown to have a tensile strength of 696.68 MPa and elastic modulus of 28.29 GPa, at a mean cross-section diameter of 46.76 μm [29].

Prasad et al. (2005) have shown that heating hemp fibers between 160°C and 260°C results in softening of lignin leading to opening of fiber bundles into individual fibers [27]. Studies show that thermal degradation of hemp fibers starts at around 150–200°C and becomes rapid at around 250°C. In their studies on thermal degradation of hemp fibers, Backermann and Pickering (2008) reported the degradation onset temperature to be 205°C [15]. Shahzad (2013) observed the weight loss behavior of hemp fiber through desiccation and at elevated temperatures. All samples were conditioned at 23˚C and 50% RH. The results showed that the

hemp fibers had equilibrium moisture content of about 10% when kept at these standard conditions [17].

Table 2-3 Properties of treated and untreated hemp fibers [28]

Hemp fiber	Untreated	NaOH			Silane		
		2%	4%	6%	2%	4%	6%
Density(g/cm^3)	1.249	1.203	1.160	1.127	1.216	1.170	1.150
Weight loss (%)		-7.99%	-9.78%	-13.58%	+0.6%	+1.08%	+2.17%
σ_t (MPa)	962.5	905.63	866	670.75	976.67	986	1025.2

Table 2-4 Properties of nanocellulose modified hemp fibers [29]

Experiment	Diameter (μm)	C.V. of diameter (%)	Modulus (GPa)	C.V. of modulus (%)	Tensile stress at break (MPa)	C.V. of stress (%)	Tensile strain at break (%)	C.V. of strain (%)
Unmodified	46.76	6.75	28.29	9.39	696.68	9.07	2.29	5.31
DTAB modification	45.10	9.65	29.83	7.95	735.29	7.65	2.47	9.98
Nanocellulose modification	51.39	7.05	38.51	8.44	1203.85	9.25	3.84	5.92

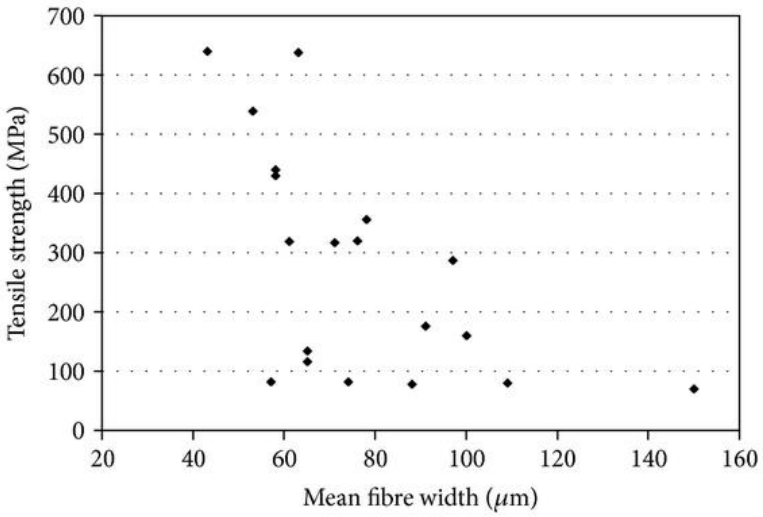

Figure 2-5 Mean cross-sectional width of hemp fibers [17]

2.2.2. Agriculture and Ecology of Hemp

Hemp is a hardy crop and can adapt to most types of environments. Although it prefers a mild climate, humid atmosphere, and a rainfall of at least 25-30 inches per year which is less than half of cotton requirements [30]. It is a natural weed suppressant and does not require herbicides or weedicides, due to rapid vegetation and formation of a canopy, which stunts any under-growth. Pest infestation of the crop is also rare and only in some cases are pesticides used, although the trend of organic farming has increased substantially in the past few years. Fertilizer requirements of hemp are N 120-140 Kg/Ha, P 30-45 Kg/Ha, K 35-60 Kg/Ha [30] for fiber type crop, depending on soil type, climate, method of agriculture, etc. The growing period of hemp for fiber is about 4-5 months.

Hemp has high yields of 7-14 Tons/Ha dry stem matter. Approximately 17% of the stalk mass is converted into useful fiber, through a process of separation of the outer bast fiber from the inner hurds (or shives), through decortication [31]. Hurds are high cellulose wood-like material, which have use in construction, mulching, compost, animal bedding, paper filling and as absorbent material [31].

2.2.3. Use and Legal Trends of Hemp

Legal cultivation of Hemp had been banned in US in 1937, which halted any advancements in technology related to the crop. Recently, however, many countries have revived the interest in the plant and many states in the US have changed their regulations. The Agricultural Act of 2014 (“farm bill,” P.L. 113-79) provided that certain research institutions and state departments of

agriculture may grow industrial hemp, as part of an agricultural pilot program, if allowed under state laws where the institution or state department of agriculture is located. The farm bill also established a statutory definition of “industrial hemp” as the plant Cannabis sativa L. and any part of such plant with a delta-9 tetrahydrocannabinol (THC) concentration of not more than 0.3% on a dry weight basis [31]. The top hemp producing countries are China, Austria, North Korea, Netherlands and Chile, with China producing 44,000 tons in 2010 [32]. This re-emergence of a versatile crop has opened up many opportunities for research and green material development. Precise data are not available on the size of the U.S. market for hemp-based products, but current industry estimates report annual sales at more than $580 million annually [31].

2.3 Polylactic Acid (PLA)

Polylactic acid (PLA) is a renewable and biodegradable thermoplastic aliphatic polyester, and is derived from resources such as corn starch, tapioca roots, chips or starch, or sugarcane. In 2010, PLA had the second highest consumption volume of any bioplastic of the world [33].

PLA thermally degrades at temperatures of about 200˚C [34] through hydrolysis, lactic reformation, oxidative main chain scission, and inter- or intramolecular transesterification. It has a glass transition temperature of about 55˚C and melting point at around 175˚C. Processing temperature for PLA is in the range of 185-190˚C [35]. Chen et al. (2003) showed the melting temperature of PLA to be 175˚C and the glass transition temperature to be around 57.4 ˚C [36]. As can be seen from Table 2-5, PLA has a tensile strength of 44-66 MPa, and modulus of 3.7 – 4.1 GPa. The impact strength of pure PLA was recorded to be 2.05 KJ/m^2 [37]. It can be processed by extrusion such as 3D printing, injection molding, film and sheet casting, and spinning, and has been used to make films, wrapping, laminates, containers, bottles, cups, toys, and other products [38]. It is known to have a melt mass flow rate of 1.5-36 g/10min, at 190˚C according to ISO 1133 [39].

Table 2-5 Properties of PLA [37]

		Annealed	
	L-PLA	L-PLA	D,L-PLA
Tensile strength (MPa)	59	66	44
Elongation at break (%)	7.0	4.0	5.4
Modulus of elasticity (MPa)	3750	4150	3900
Yield strength (MPa)	70	70	53
Flexural strength (MPa)	106	119	88
Unnotched izod impact (J/m)	195	350	150
Notched izod impact (J/m)	26	66	18
Rockwell hardness	88	88	76
Heat deflection temperature (°C)	55	61	50
Vicat penetration (°C)	59	165	52

2.4 Non-Woven Natural Fiber Composites

Chen et al. (2012) fabricated Kenaf/Polypropylene composites in the weight ratio 50/50 and tested mechanical properties for different hot compression molding parameters. The non – woven felts were made by a carding process followed by needle punching [40]. They concluded that samples which were processed at higher temperature (230˚C) but shorter time (60 s) had the best mechanical performance, with the highest tensile modulus 1536 MPa and highest tensile failure strain 1.5 % [40]. They also found that the molding pressure shows no significant effect on the composite moduli. A stress-strain graph from Figure 2-6 shows the tensile strength at yield of the material to be around 14 MPa.

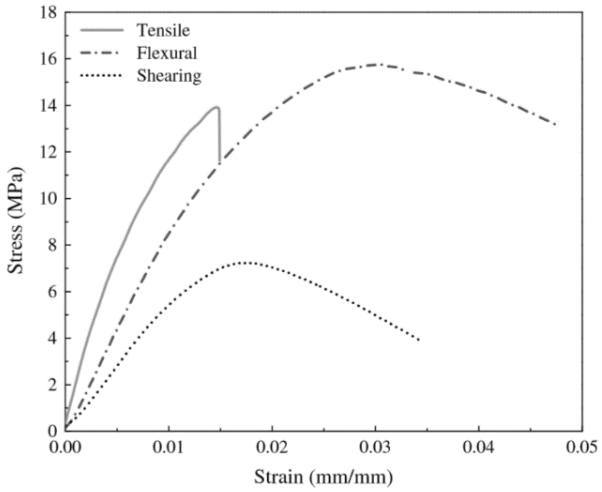

Figure 2-6 Stress vs Strain of kenaf/PP composite [40]

Table 2-6 Properties of kenaf/PP composites at different compression molding parameters [48]

Sample ID	Tensile modulus (MPa)	Flexural modulus (MPa)	In-plane shear modulus (MPa)	Impact strength (kJ/m^2)	Poisson's ratio
5/230/120	424(25)	306(11)	172(10)	2.94(0.45)[b]	0.23
5/230/60	347(21)	183(5)	139(8)	3.33(0.69)[b]	0.25
5/200/120	323(8)	177(6)	130(4)[a]	3.98(0.63)	0.25
5/200/60	300(15)	158(14)	124(5)[a]	9.70(0.85)	0.21
7/230/120	395(13)	356(28)	165(6)	3.16(0.28)	0.20
7/230/60	366(19)	273(22)	150(10)	3.78(0.64)[c]	0.22
7/200/120	340(6)	150(16)	135(10)	3.64(0.36)[c]	0.26
7/200/60	262(6)	108(13)	101(8)	9.00(1.70)	0.30

Hao et al. (2013) fabricated kenaf/PP composites, whose properties can be seen in Table 2-6. The samples IDs are of the form X/Y/Z, where X is pressure (bar), Y is temperature (˚C) and Z is time (sec). The tensile modulus ranges from 262 MPa to 424 MPa and the impact strengths range from 2.94 KJ/m^2 (0.294 J/cm2) to 9.70 KJ/m^2 (0.97 J/cm^2) [48]. Another study, by Chen Y. (2005), that was based on kenaf-polypropylene (KP), bagasse-polypropylene (BP) and ramie-polypropylene (RP) composites, reported mean values for their respective tensile strengths were 17.039 MPa, 7.634 MPa and 11.783 MPa respectively and modulus were 327.237 MPa, 180.848 MPa and 317.719 MPa respectively [41]. N. Martin et al. (2016) fabricated non-woven flax/PP composites using three different mat manufacturing methods – spun-lacing, needle punching and paper processing, at varied fiber loading levels. MAPP (maleic anhydride polypropylene) was used as coupling agent for better fiber polymer adhesion. They reported a maximum tensile strength of 93 MPa and modulus of 9569 MPa for paper processed mats at nearly 40% fiber loading [42]. Yuan Jian and Isaac (2007) tested tensile properties of hemp/Polyester composites formed by hand lay-up method at different curing pressures. They recorded a high tensile strength of 53 MPa and modulus of 6.2 GPa [43]. This was comparable to glass fiber/polyester properties measured at 43 MPa tensile strength and 5.9 GPa modulus [43].

Uawongsuwan et al. recorded the impact energies for bamboo, vetiver grass and coconut fiber reinforced PLA composites and found that bamboo fiber composites had the greatest impact energy of 1.56 KJ/m^2 [44]. Jawaid et al. (2011) tested sandwich composites made of jute (J) and oil palm empty bunch fibers (EFB) with epoxy as the matrix. EFB/J/EFB and J/EFB/J fiber mats were used, without coupling agents, and the impact strength was found to be 15 kJ/m^2 (1.5

J/cm^2) and 6.42 kJ/m^2 (0.642 J/cm^2), respectively. But when 2-hydroxy ethyl acrylate as used as the coupling agents (CA), these values is increased to 19.47 kJ/m^2 (1.95 J/cm^2) and 7.32 kJ/m^2 (0.73 J/cm^2) respectively [45]. Zampaloni et al. (2007) documented that Kenaf/PP composites at 40% fiber loading showed impact strengths of 3.9 J/cm^2 [46]. Pickering et al. (2016) reviewed impact strengths of various natural fiber composites and recorded that wood fibers/PP composites at 40% had an impact strength of around 4.0 J/cm^2 and Hemp/PP composites coupled with MAPP had impact strengths of 21 J/cm^2 [47].

Chen et al. (2012) performed thermal gravimetric analysis of the kenaf/PP composites and showed that for kenaf fiber, the main thermal decomposition in N2 (60% mass fraction) occurred within 272.6–446.5˚C [48]. This was due to the decomposition of cellulose, which is the major component of kenaf fiber (44–57%). The decomposition of PP fiber happened within 344.4˚C – 425.3˚C. However, in the air atmosphere, the decomposition temperature T90% (10% weight loss) was almost the same for both kenaf and PP fiber, until at T30% (360˚C) where the kenaf weight loss rate begins slowing down, most probably because of the need of high temperature to decompose lignin. Overall, for both kenaf and PP fiber, T30% was higher in N2 than in air, indicating that the thermal decomposition is more efficient with the presence of oxygen [48]. DMA tests showed that the highest sample had a glass transition temperature of 46.3˚C and melting temperature of 158.1˚C and lowest sample had a glass transition temperature of 43.7˚C and melting temperature of 160.1˚C [48]. Chen Y. (2005) performed DMA analysis on the BP, KP, and RP composites and the tan δ (ratio of the loss-to-storage moduli) curve showed that the mean softening temperature was about 140˚C and the melting point to

lose the tensile strength was about 160˚C [41]. Behzad and Sain (2007) measured thermal conductivities for hemp/acrylic resin composites to be around 0.25 W/m-K at 50% fiber loading [49]. Osugi et al. (2009) prepared composites made of manila hemp and PLA and observed a thermal conductivity of about 0.24 W/m-K at 50% fiber loading and 0.2 W/m-K near 70% fiber loading. [50]. The thermal conductivity values for some plastics are mentioned here– LDPE 0.33 W/m-K, HDPE 0.5 W/m-K, epoxy 0.17 W/m-K, Nylon6 0.25 W/m-K, PVC 0.19 W/m-K, PLA 0.13 W/m-K [51]. These are the most widely used plastics in automobiles and are applied to trim panels, body panels, roof panels, HVAC, fenders, trunk liners, upholstery and other low - structural areas.

Hao et al. (2013) recorded the acoustic absorption coefficients of samples 7/200/60 and 5/200/60 to be as high as 0.93 and 0.88 at 6400Hz respectively [48], as shown in Figure 2-7. Chen et al. (2010), performed experiments on spun-laced flax/polypropylene felts and composites. The sample numbers #4 and #5 refer to two different water pressure settings for the spun lacing process. The two microphone impedance tube measurement test was used to characterize the acoustic absorption and the transmission loss tube method for testing sound insulation properties of the composite. They found that for both the high (~6.5 KHz) and low frequency (50 Hz) range the absorption coefficient was near to or less than 0.3 [52]. Figure 2-9 shows the absorption coefficients for the felt and composites samples. Sound insulation properties were also tested and the results are shown in Figure 2-10. It was shown that the composite panels had better insulation properties, which is a feature of a typical isotropic panel

[52]. Also, the higher water pressure setting enhanced the transmission loss property of the material.

Koenig and Mueller tested acoustical properties of Hemp-PP composites, fabricated with varying fiber mat compactness or density. Impedance tube tests gave the results shown in Figure 2-8. No difference can be seen for composites in the low frequency range beneath 1 kHz. In the frequency range between 1 and 2 kHz, strongly compacted composites show the lowest absorption. However, for higher frequencies this influence inverses as above a frequency of 2 kHz highly compacted composites show the best absorption values [53].

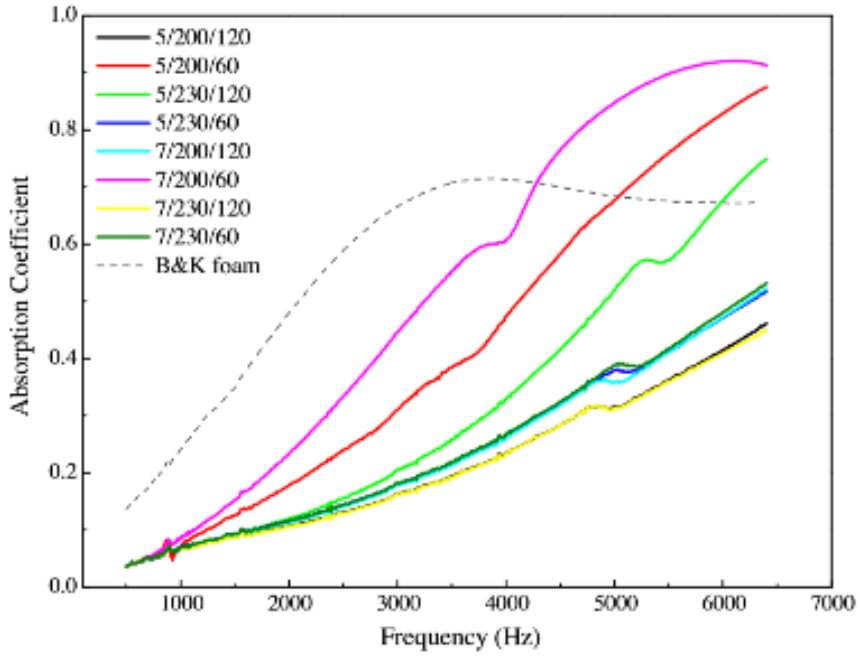

Figure 2-7 Absorption coefficient of kenaf/PP samples [48]

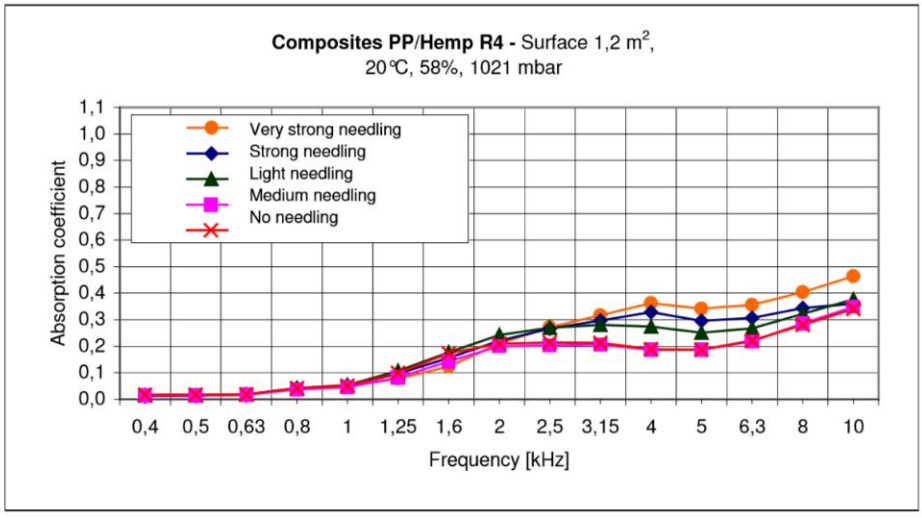

Figure 2-8 Acoustic absorption coefficient of hemp/PP samples [53]

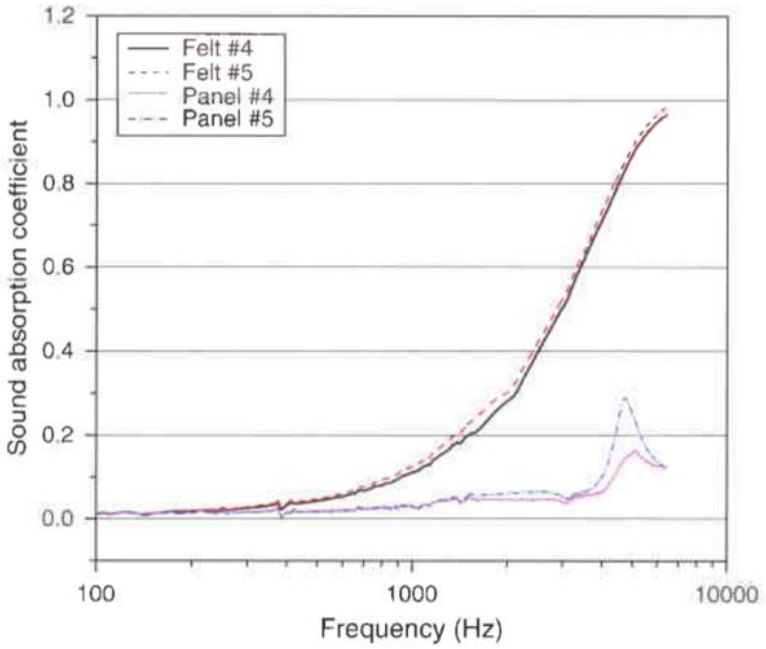

Figure 2-9 Acoustic absorption coefficient of hemp/PP felts and composites [52]

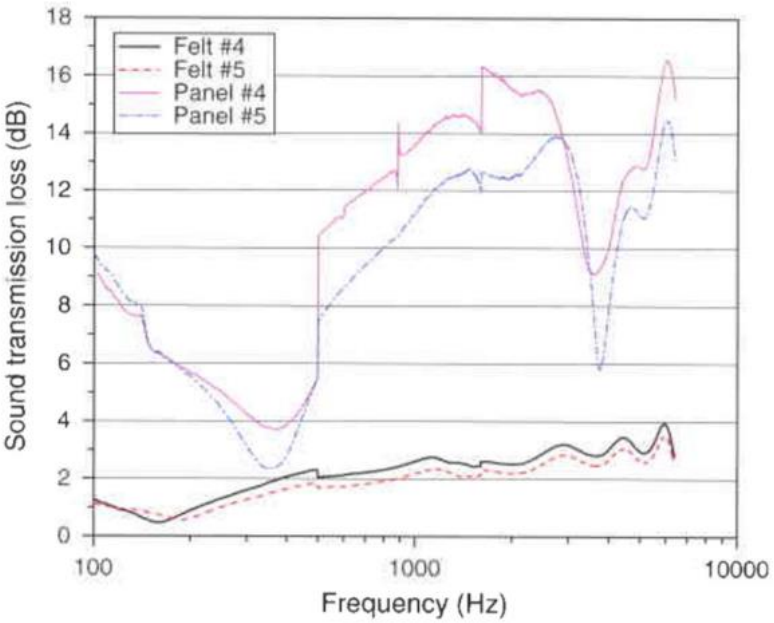

Figure 2-10 Acoustic transmission coefficient of hemp/PP felts and composites [52]

Chapter 3 Experimentation

The research presented here is based on non-woven hemp-PLA composites prepared using a hemp fiber mat and PLA powder, through carding and needle punching processes, followed by hot compression molding. The purpose was to characterize the composite material based on mechanical, thermal and acoustic properties. The experimentation was broken up into three parts – (i) identify and validate proper hemp-PLA felt fabrication procedure, (ii) identify proper compression molding parameters and (iii) fabricate samples based on varying fiber loading for characterization. A novel method for preparing the composite is tested here, where the PLA, in powder form, is iteratively spread over the hemp felt between needle punching rounds (Figure 3-1). It was speculated that the needle punching process would help disperse the PLA powder throughout the thickness of the felt, with reasonable PLA loss. The PLA lost, however, could easily be recovered for reuse.

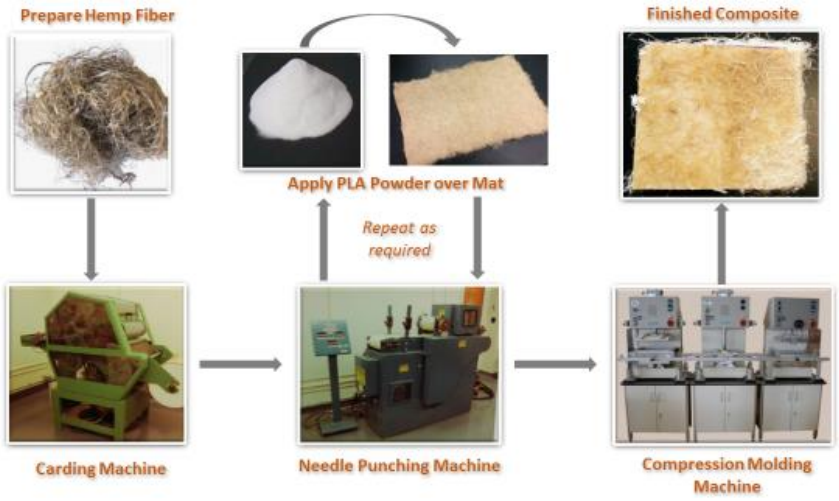

Figure 3-1 Schematic representation of process of composite fabrication

3.1 Materials and Equipment

Hemp fiber

The hemp fiber was obtained from HempTraders, Inc. based in Paramount, California. The company sells hemp fibers and a range of hemp products commercially. Hence, the hemp fibers used in the research can be assumed to be of a scalable quality and quantity. Raw long hemp fiber were used and the length varied from 3 in to 36 in. The fiber was field retted with a shive content of less than 1%. (Shive content is the percentage (by weight) of shives (or hurds) in the retted fibers). The width of the fibers varied as they were not fully separated. No extra processing was done on the fibers.

Figure 3-2 Hemp fiber for experiment

PLA

The PLA powder used was named ECOSCRUB 20PC purchased from Micro Powder, Inc. (Figure 3-3). The melting range was specified to be between 140˚C - 150˚C, the density, at 25˚C, was 1.23-1.25 g/cm^3 and the maximum particle size was 840 microns.

Figure 3-3 PLA powder for experiment

Carding machine

Carding is a mechanical process that disentangles, cleans and intermixes fibers to produce a continuous web suitable for subsequent processing. This is achieved by passing the fibers

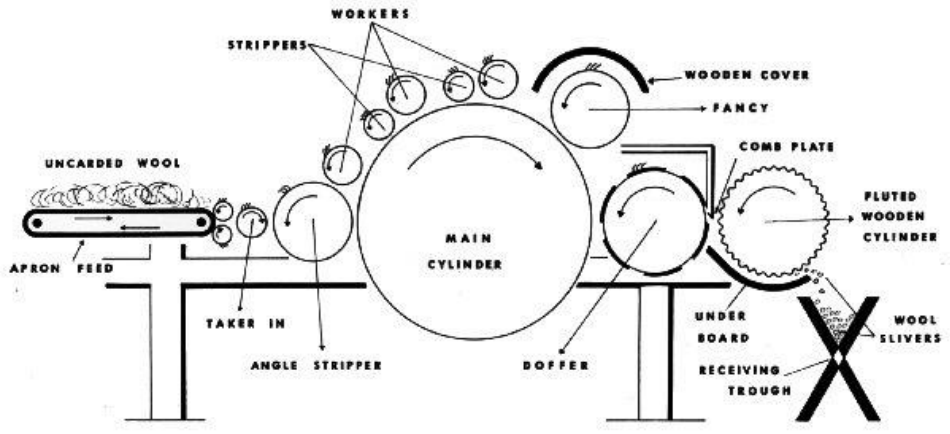

Figure 3-4 Schematic of carding process

between differentially moving surfaces covered with card clothing. It breaks up locks and unorganized clumps of fiber and then aligns the individual fibers to be parallel with each other [54]. Figure 3-4 shows the schematic cut-away of a typical carding machine.

Needle punching machine

Needle punching is a method used to produce non-woven felts from fiber mats. The fiber mat are punched through by barbed needles, which entangles some of the top layer fibers with the lower layers and vice versa. This needling action interlocks fibers, which are held together by friction forces, producing a consolidated fiber felt. Figure3-5 shows the schematic working of a

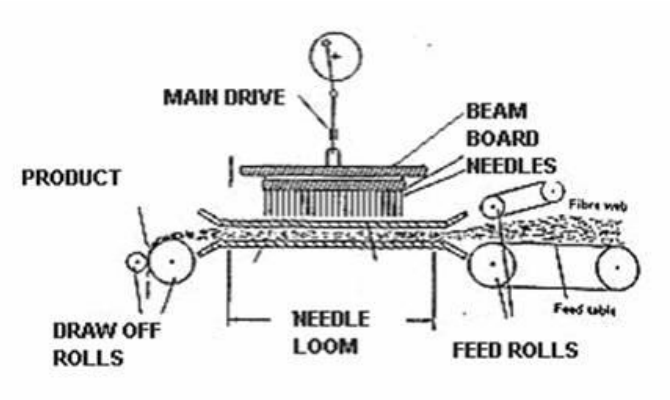

Figure 3-5 Cross sectional schematic of needle punching machine

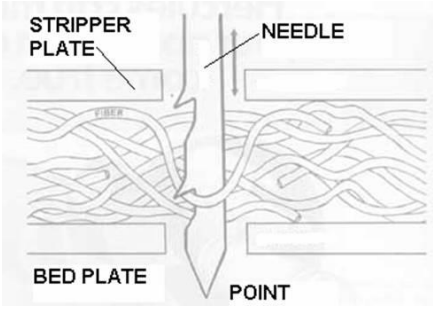

Figure 3-6 Close up of needling action

needle punching machine. The rate of needle punching used for the experiments was 229 strokes/min and feeding speed was 1.6 m/min.

Compression molding apparatus

A Maschinenfabrik Herbert Meyer GmbH laboratory APV press Model IR3530 was used for compression molding of the samples. The rated press force is 14KN with pneumatic pressure generation, and the heating plate's heat to a maximum of 400˚C.

Figure 3-7 Maschinenfabrik Herbert Meyer GmbH laboratory APV press Model IR3530 for compression molding

Tensile testing machine

An Instron model 5966 was used for tensile testing. It has a 10KN load capacity, with load measurement accuracy of +/- 0.5% of reading. Testing speed can range from form 0.001 – 3000 mm/min.

Figure 3-8 Instron model 5966 tensile testing machine

Impact testing machine

The impact strength was tested on an Izod Impact Tester manufactured by Shanta Engineering (Figure 3-9). The apparatus' maximum available energy is 21.68 Joules. They also provide a Motorized Notch Cutter (Figure 3-10) specified to ASTM D256 standards for sample preparation.

Figure 3-9 Izod Impact testing apparatus

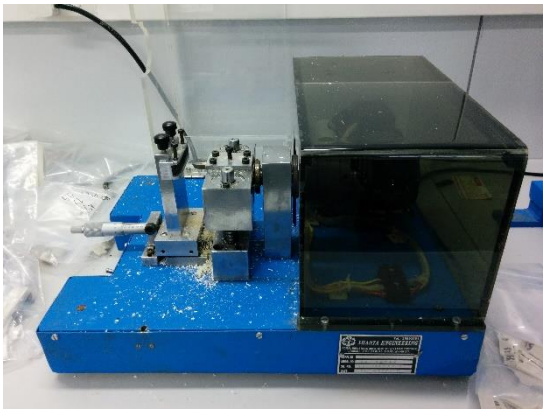

Figure 3-10 Motorized notch cutter

Acoustic testing apparatus

The Brüel & Kjær Impedance Measurement Tubes Type 4206 apparatus was used to test for normal acoustic absorption, using the Two Microphone Method. The Transmission Loss Tube Type 4206T apparatus was used for measuring normal transmission loss properties, using the Four Microphone Method. Both setups consist of large and small tubes corresponding to low and high frequency measurements, respectively.

The two microphone transfer function method

A sound source is mounted at one end of the impedance tube and a sample of the material is placed at the other end (Figure 3-2). The loudspeaker generates broadband, stationary random sound waves. These propagate as plane waves in the tube, hit the sample and are reflected. Therefore, a standing-wave interference pattern results due to the superposition of forward- and backward-travelling waves inside the tube. By measuring the sound pressure at two fixed locations and calculating the complex transfer function using a two-channel digital frequency

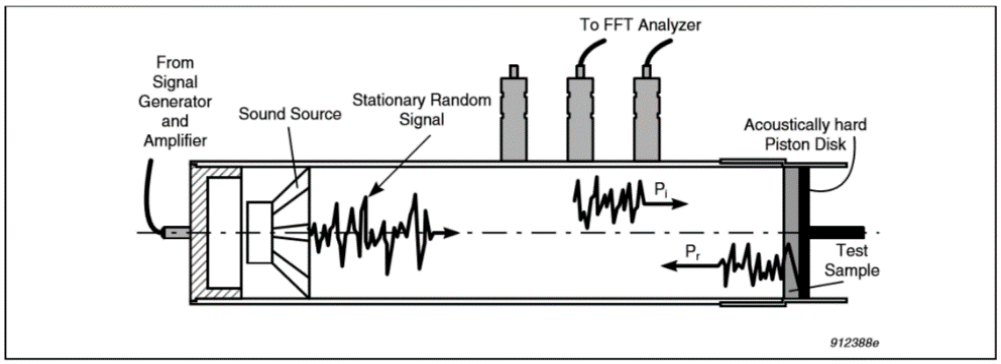

Figure 3-11 Cut away diagram of impedance measurement tube, showing incident and reflected components of stationary random signal

analyzer, it is possible to determine the complex reflection coefficient, the sound absorption coefficient and the normal acoustic impedance of the material. The usable frequency range depends on the diameter of the tube and the spacing between the microphone positions.

The four-microphone transfer-function method

A sound source is mounted at one end of the impedance tube and a sample of the material is placed in a holder (Figure 3-4). The loudspeaker generates broadband, stationary random sound waves that propagate as plane waves. The plane waves hit the sample in the holder with part of the wave reflected back into the source tube, part absorbed by the material, and part passing through the material to the receiving tube. The portion of the plane wave that passes through the material then encounters the end of the receiving tube where some of it is reflected and some exits the tube. By measuring the sound pressure at four fixed locations (two in the source tube and two in the receiving tube) and calculating the complex transfer function using a four-channel digital frequency analyzer, it is possible to determine the transmission loss of the material. The usable frequency range depends on the diameter of the tube and the spacing between the microphone positions.

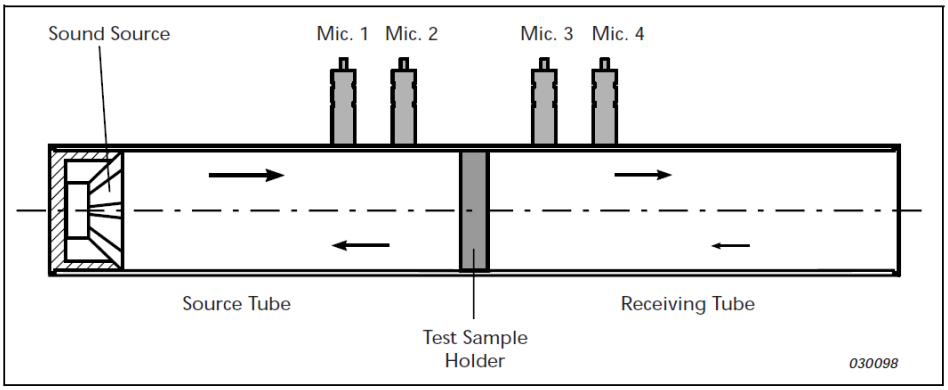

Figure 3-12 Cut away of transmission loss tube

Dynamic mechanical analysis machine

The DMA Q800 model by TA Instruments was used for dynamic mechanical analysis (Figure 3-13). It uses non-contact linear drive technology which provides precise control of stress, and air bearings for low friction support. Strain is measured using optical encoder technology, which provides high sensitivity and resolution. It has a temperature range from -150˚C to 600˚C at heating rates from 0.1 to 20 ˚C/min and can provide a maximum force of 18N.

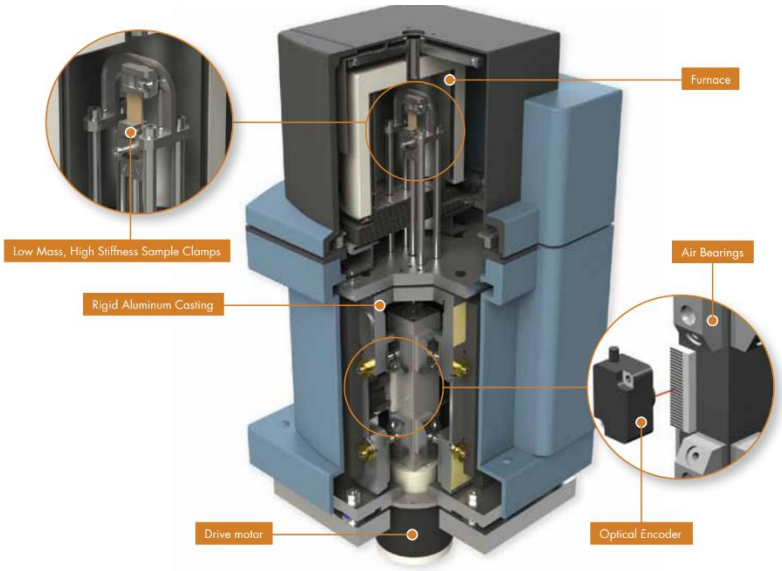

Figure 3-13 DMA Q800

Thermal conductivity setup

A Guarded Hot-Plate Apparatus, with ASTM C1044-07 standard practice, was used for assessing thermal conductivity values of the composite samples. The schematic setup can be seen in Figure3-14. An auxiliary insulation, 3.2mm thick, with a thermal conductivity (k) value of 0.036

W/m-K at 25 ºC, 0.038 W/m-K at 93 ºC, and 0.046 W/m-K at 204 ºC was used to prevent heat flow in opposite direction. The effective heating area was 3.04×10^{-4} m^2.

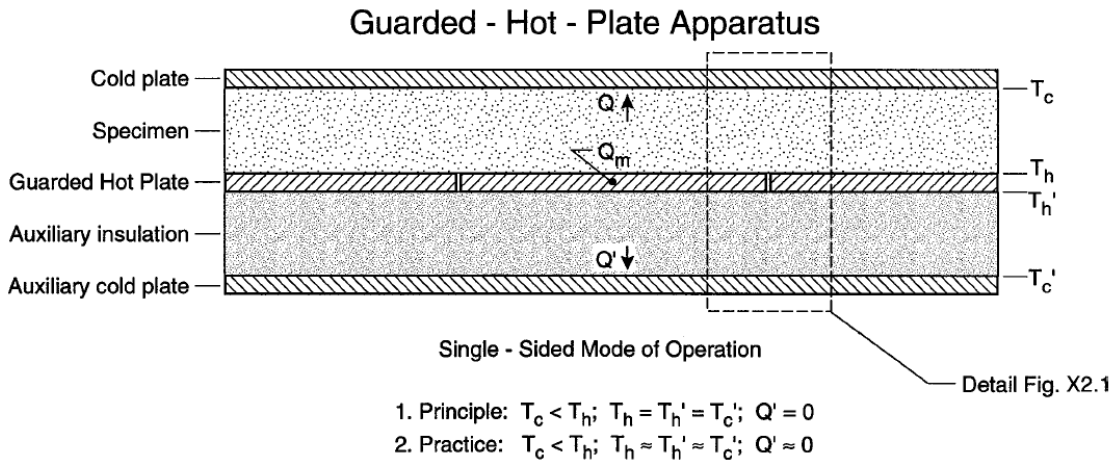

Figure 3-14 Schematic of thermal conductivity measurement setup

Th` : Temperature of top of guarded hot plate

Tc` : Temperature of auxiliary cold plate

Th : Temperature of top surface of guarded hot plate

Tc : Temperature of cold plate

3.2 Felt Fabrication Procedure

Trials were run to determine the procedure for hemp fiber/PLA felt fabrication and estimate the PLA lost through each round of needle-punching. Six trials were run, each starting with 100g of hemp fiber loosely separated and cut down to lengths of 5-10 cm by scissors.

The hemp fiber mats were made by passing 100g of fiber through the carding machine. The first three samples were carded for 3 rounds and the second three samples were carded for 4 rounds. The mats produced were weighed to check for fiber loss during carding and to record the fiber input weight for the needle punching process.

The next step was needle punching. Needle punching interweaves the fibers in the mat creating a compacted felt. The compactness and density of the felt depends on the number of rounds of needle punching. For the needle punching process, different variations of number of rounds, addition of PLA and folding of the felt were used. The general procedure consisted of sprinkling a layer of PLA over the fiber, by hand, and passing through the needle punching machine. The felt was folded over and more PLA was added, as required by the fiber loading, and again needle punched. This process was repeated until the desired thickness and density of composite felt was achieved. The total PLA added was equal to the fiber mat weight, to achieve 50% fiber loading. The complete procedures of felt fabrication can be seen in Table3-1. The sample hemp/PLA felts made were named S1, S2, S3, S4, S5 and S6.

Table 3-1 Felt fabrication procedure

Sample #				Before Operation			After Operation					
S1	**Process**	**#Round**	**Operation**	**PLA Added (gms)**	**Total PLA Added (gms)**	**Input Weight(gms)**	**Output Weight(gms)**	**PLA Lost (gms)**	**Total PLA lost (gms)**	**PLA Left (gms)**	**Ratio(HF/PLA)**	**PLA Loss %**
	Carding	1				100.0						
		2										
		3					63.5					
	Needle Punching	1	Mat from Carding	0.0	0.0	63.5	63.5	0	0	0	0.00	0.00
		2	Fold/add PLA half	31.7	31.7	95.2	81.6	13.6	13.6	18.1	3.51	42.90
		3	Fold/add PLA half	31.7	63.4	113.3	111.3	2.0	15.6	47.8	1.33	24.61
		4	Go	0.0	63.4	111.3	107.8	3.5	19.1	44.3	1.43	30.13
		5	Go	0.0	63.4	107.8	104.9	2.9	22.0	41.4	1.53	34.70
		6	Go	0.0	63.4	104.9	102.0	2.9	24.9	38.5	1.65	39.27
		7	Flip/Go	0.0	63.4	102.0	98.3	3.7	28.6	34.8	1.82	45.11
		8	Go	0.0	63.4	98.3	96.4	1.9	30.5	32.9	1.93	48.11
		9	Go	0.0	63.4	96.4	96.3	0.1	30.6	32.8	1.94	48.26
		10	Flip/Go	0.0	63.4	96.3	95.0	1.3	31.9	31.5	2.02	50.32
S2	**Process**	**#Round**	**Procedure**	**PLA Added (gms)**	**Total PLA added (gms)**	**Input Weight(gms**	**Output Weight(gms)**	**PLA Lost (gms)**	**Total PLA lost (gms)**	**PLA Left (gms)**	**Ratio(HF/PLA)**	**PLA Loss %**
						100.0						
	Carding	1										
		2										
		3					74.3					
	Needle Punching	1	Mat from carding	0.0	0.0	77.3	76.6	0.0	0.0	0.0		0.00
		2	Fold/Add half PLA	38.3	38.3	115.6	104.5	11.1	11.1	27.2	2.82	28.98
		3	Fold/Add half PLA	38.3	76.6	142.8	142.2	0.6	11.7	64.9	1.18	15.27
		4	Reverse Go	0.0	76.6	142.2	140.2	2.0	13.7	62.9	1.22	17.89
		5	Go	0.0	76.6	140.2	139.1	1.1	14.8	61.8	1.24	19.32
		6	Flip/Go	0.0	76.6	139.1	127.3	11.8	26.6	50.0	1.53	34.73
		7	Flip/Go	0.0	76.6	127.3	126.8	0.5	27.1	49.5	1.55	35.38
S3	**Process**	**#Round**	**Procedure**	**PLA Added (gms)**	**Total PLA added (gms)**	**Input Weight(gms**	**Output Weight(gms)**	**PLA Lost (gms)**	**Total PLA lost (gms)**	**PLA Left (gms)**	**Ratio(HF/PLA)**	**PLA Loss %**
						100.0						
	Carding	1										
		2										
		3					71.0					
	Needle Punching	1	Mat from carding	0.0	0.0	71.0	59.4	0.0	0.0	0.0		0.00
		2	Add quart PLA/Fold/Add quart PLA	26.2	26.2	85.6	81.0	4.6	4.6	21.6	2.75	17.56
		3	Fold/Add half PLA	33.2	59.4	114.2	110.8	3.4	8.0	51.4	1.16	13.47
		4	Reverse Go	0.0	59.4	110.8	109.5	1.3	9.3	50.1	1.19	15.66
		5	Go	0.0	59.4	109.5	108.4	1.1	10.4	49.0	1.21	17.51
		6	Go	0.0	59.4	108.4	107.3	1.1	11.5	47.9	1.24	19.36
		7	Go	0.0	59.4	107.3	106.2	1.1	12.6	46.8	1.27	21.21
S4	**Process**	**#Round**	**Procedure**	**PLA Added (gms)**	**Total PLA added (gms)**	**Input Weight(gms)**	**Output Weight(gms)**	**PLA Lost (gms)**	**Total PLA lost (gms)**	**PLA Left (gms)**	**Ratio(HF/PLA)**	**PLA Loss %**
						100.0						
	Carding	1										
		2										
		3										
		4					71.5					
	Needle Punching	1	Mat from carding	0.0	0.0	71.5	69.3	0.0	0.0	0.0		0.00
		2	Fold/Add half PLA	34.6	34.6	106.1	100.4	5.7	5.7	28.9	2.40	16.47
		3	Fold/Add half PLA	34.6	69.2	135.0	130.7	4.3	10.0	59.2	1.17	14.45
		4	Reverse Go	0.0	69.2	130.7	129.3	1.4	11.4	57.8	1.20	16.47
		5	Go	0.0	69.2	129.3	127.8	1.5	12.9	56.3	1.23	18.64
		6	Go	0.0	69.2	127.8	126.8	1.0	13.9	55.3	1.25	20.09
		7	Go	0.0	69.2	126.8	126.1	0.7	14.6	54.6	1.27	21.10
		8	Go	0.0	69.2	126.1	125.8	0.3	14.9	54.3	1.28	21.53
		9	Go	0.0	69.2	125.8	125.2	0.6	15.5	53.7	1.29	22.40
3/25/2016												
S5	**Process**	**#Round**	**Operation**	**PLA Added (gms)**	**Total PLA Added (gms)**	**Input Weight(gms)**	**Output Weight(gms)**	**PLA Lost (gms)**	**Total PLA lost (gms)**	**PLA Left (gms)**	**Ratio(HF/PLA)**	**PLA Loss %**
						100.0						
	Carding	1										
		2										
		3										
		4					69.9					
	Needle Punching	1	Mat from Carding	0.0	0.0	69.9		0	0	0		
		2	Go	0.0	0.0	69.9	68.5	0.0	0.0	0.0		
		3	Fold/add PLA half	34.3	34.3	102.8	99.6	3.2	3.2	31.1	2.25	9.20
		4	Fold/add PLA half	34.3	68.6	133.9	131.5	2.4	5.5	63.0	1.11	8.10
		5	Go	0.0	68.6	131.5	130.4	1.2	6.7	61.9	1.13	9.77
		6	Go	0.0	68.6	130.4	129.5	0.8	7.5	61.0	1.15	11.01
		7	Go	0.0	68.6	129.5	129.0	0.5	8.0	60.5	1.16	11.74
S6	**Process**	**#Round**	**Operation**	**PLA Added (gms)**	**Total PLA Added (gms)**	**Input Weight(gms)**	**Output Weight(gms)**	**PLA Lost (gms)**	**Total PLA lost (gms)**	**PLA Left (gms)**	**Ratio(HF/PLA)**	**PLA Loss %**
						100.0						
	Carding	1										
		2										
		3										
		4					68.4					
	Needle Punching	1	Mat from Carding	0.0	0.0	68.4	65.7	0	0	0		
		2	Go	0.0	0.0	65.7	65.7	0.0	0.0	0.0		
		3	Add PLA half	32.9	32.9	98.6	88.5	10.1	10.1	22.8	3.00	30.70
		4	Fold/add PLA half	32.9	65.8	121.4	114.6	6.8	16.9	48.9	1.40	25.68
		5	Go	0.0	65.8	114.6	111.3	3.3	20.2	45.6	1.50	30.70
		6	Go	0.0	65.8	111.3	108.9	2.4	22.6	43.2	1.58	34.35
		7	Go	0.0	65.8	108.9	106.9	2.0	24.6	41.2	1.66	37.39

3.3 Compression Molding Parameters

The compression molding parameters depend on the properties of the input materials. The goal is to achieve complete and uniform melting and penetration of the PLA powder throughout the fiber felt, hence maximizing contact and adhesion between fiber and polymer. No coupling agent or compatibilizer was used to aid in the bonding, which could have major effects on the strength of the material.

Keeping in mind the PLA melting point to be at 175˚C, processing temperatures of about 185-190˚C [35], and the thermal degradation onset of hemp fiber to be at around 205˚C [55], two levels for the temperature processing range, for testing, were set at 180˚C and 190˚C. Based on previous works by Chen et al. (2012), processing pressure was fixed at 5 bar, as its change has little to no impact on the composite properties. The time of compression was tested for two levels: 100 sec and 120 sec, based on previous works [40] and the melt flow properties of PLA [39]. Each sample, from S1 to S6, was cut into four strips and compression molded for the four different processing conditions, as shown in Table 3-2. After compression molding, each sample was cooled under 1 bar pressure for 100 seconds, to give the surface a good finish.

The samples were denoted “SxTy”, where ‘x’ is the felt sample number and ‘y’ is the trial number.

Table 3-2 Processing parameters for compression molding

Trial	Press (Bar)	Temp (deg C)	Time (sec)
1	5	180	100
2	5	180	120
3	5	190	100
4	5	190	120

3.4 Final Sample Preparation and Characterization

Once the compression molding processing parameters were found, the final samples were prepared to test for characterization. The process for felt fabrication, through carding and needle punching, was kept consistent for all the samples. Appendix A-1 shows the detailed procedure for the final sample hemp/PLA felt fabrication. Six different samples were made - three at 55% fiber loading, two at 50% fiber loading and one at 35% fiber loading. These three wt%'s correspond to HF/PLA ratios of 1.23, 1.00 and 0.50. Since the fiber mat from the carding machine is not perfectly consistent, some samples required an additional 9th round of needle punching for uniform thickness. However, this extra round does not affect PLA loss as stated previously, and can be seen in Figure 3-16.

The compression molding processing parameters of the samples were kept consistent at 190˚C at 5 bar pressure for 120 seconds, from the results in Section 4.2. These composite panels were used to create samples required for testing and were named 1, 2, 3, 4, 5, and 6. All other test specimens were cut out of these panels. The composite panels had minimal residual PLA and were mostly uniform over the area. The top surface had a hard and shiny finish and the bottom surface was fibrous (Figure 3-15).

Figure 3-15 Final sample panel: plastic surface (left), fibrous surface (right)

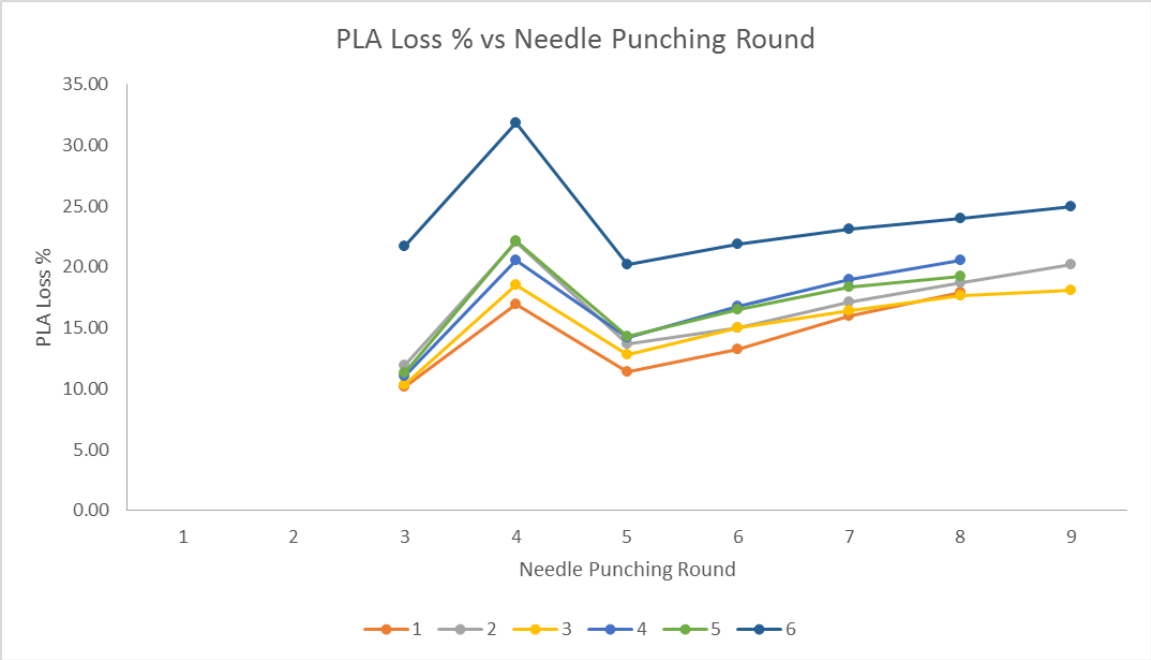

Figure 3-16 Final Samples: PLA loss % vs. Needle Punching round

3.4.1 Tensile Test

The Instron model 5966 tensile testing machine was used with the ASTM D3039 standards for composite materials. Rectangular specimens of size 6 in x1 in (152.4mm x 25.4 mm) with an average thickness of 0.15 in (3.69 mm) were made, using a desktop band saw. Three replicates were used for each of the six samples (Figure 3-17). The samples were conditioned at 21˚C and 65% RH for 48 hours. They were named “xTy”, where ‘x’ is the sample number and ‘y’ is the replicate number. The gage length was 3 in (76.2mm) and a load cell of 10 KN was applied at a speed of 2 mm/min.

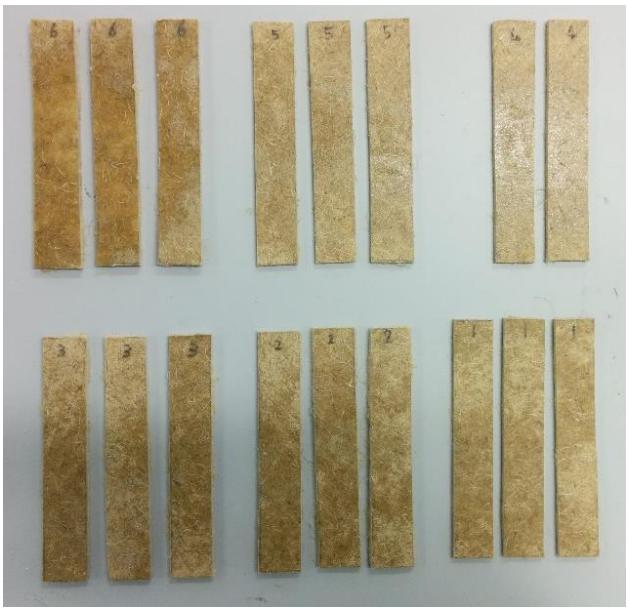

Figure 3-17 Sample specimens for tensile testing

3.4.2 Impact Test

The ASTM D256-10 standard was used to test the notched impact strength of the composites. The test specimens were rectangular with 63.5 mm x 12.7 mm (2.5 in x 0.5 in) and a mean thickness of 3.45 mm (Figure 3-18). The specimen geometry is shown in Figure 3-19. The notches were made on the motorized notch cutter. Two replicates for each sample were conditioned at 21˚C and 65% RH for 48 hours. The breaking energy was recorded in J/cm^2. The samples were named “Ix” where x is the sample number.

Figure 3-18 Sample specimens for impact testing

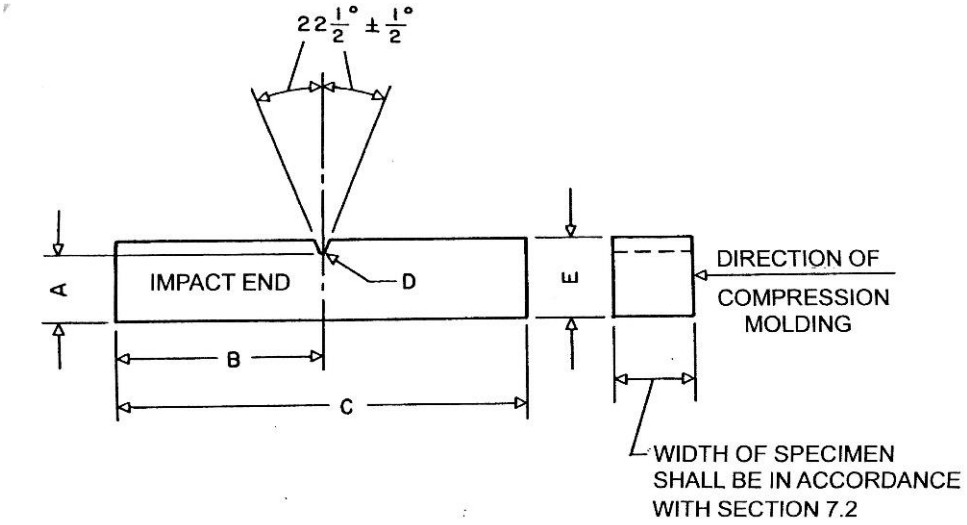

	mm	in.
A	10.16 ± 0.05	0.400 ± 0.002
B	31.8 ± 1.0	1.25 ± 0.04
C	63.5 ± 2.0	2.50 ± 0.08
D	0.25R ± 0.05	0.010R ± 0.002
E	12.70 ± 0.20	0.500 ± 0.008

Figure 3-19 Measurements for impact testing samples

3.4.3 Acoustic Tests

The Brüel & Kjær Impedance Measurement Tubes Type 4206 apparatus was used to test for acoustic absorption and insulation properties of the composites. Two different sizes were used – large tunnel and small tunnel, corresponding to low frequency range (50Hz – 1.6KHz) and higher frequency range (500Hz - 6.4KHz), respectively. The large tube required circular specimens of diameter 3.9in (100mm) and small tube required a diameter of 1.1in (29mm), which were made by stamping of the composite panel samples. Six individual specimens were prepared representing each sample, for both frequency range tests, named 1, 2, 3, 4, 5 and 6 (Figure 3-20). The average thickness was approximately 3.34mm. Different setups are required for absorption coefficient measurement and acoustic transmission loss, as previously discussed.

Figure 3-20 Samples for acoustic testing: low frequency (left), high frequency (right)

Acoustic Absorption Coefficient

The PULSE Labshop Version 13 for Material Testing software was used for absorption coefficient measurements. The setup was first calibrated using a provided calibration sample, with the following limits – Signal to Noise ratio above 10dB and Calibration Factors within +/- 2dB. The environment settings were 101.325KPa atmospheric pressure, 20˚C ambient temperature and 80% RH. The low frequency measurements, using the large tube, were made first. All the samples were tested successively with the fibrous surface facing the sound source. The procedure was repeated once. They were named "RxLy", where 'x' denotes round of testing and 'y' is the sample number. Next, all the samples were tested with the plastic surface facing the sound source, and were named "RevLy" where y is the sample number. This whole procedure was repeated for the high frequency/small tube, measurements and the samples were named "RxSy", for fibrous surface facing the sound source, and "RevSy", for the reversed sample.

3.4.4 Dynamic Mechanical Analysis

The DMA Q800 apparatus was used to characterize the dynamic modulus and glass transition temperature of the composites. Film tension type clamps were used and the samples were sized accordingly – 40mm x 12mm with an average thickness of 3.77mm (Figure 3-21). Out of the several modes of operation available, the Multi-frequency temperature-sweep mode was used. The poisson ratio was set at 0.44, for plastics, and a preload force of 0.01N was applied. The temperature ramp speed was set at 4˚C/mm, and measurements were made at a single frequency of 1KHz. Each sample was tested for temperature ranging from about 25˚C to 120˚C.

Figure 3-21 Specimens for DMA testing

3.4.4 Thermal Conductivity

The setup required square samples of side 1.25 in (31.75 mm). The average thickness of the samples used was 3.74 mm (Figure 3-22). The current and voltage input were varied to reach steady state temperatures near 50˚C, 60˚C, 70˚C, 80˚C and 90˚C. The Th` and Tc` measurement, with the provided value of C` were used to calculate the heat flow rate through the insulation material, Q`, using:

$$Q` = C`A(T_c` - T_h`)$$

The heat flow rate through the sample is given by:

$$Q = Q_m - Q'$$

Where Q_m (W) is determined by current and voltage input. The thermal conductivity was found from:

$$C = \frac{k}{l}$$

Where l is the thickness. The thermal conductivity values (W/m-K) were recorded and tabulated for the given temperatures.

Figure 3-22 Specimens for thermal conductivity measurements

Chapter 4 Results and Discussion

4.1 Felt Fabrication Results

The carding process lead to an average loss of 30.24% of hemp fibers. No significant difference was observed based on the rounds of carding. The felts produced were of similar fiber lengths and densities as could be observed by inspection and weighing. It was decided to opt for four rounds of carding for final sample preparation.

Each of the six samples went through unique needle punching processes as stated previously (Table 3-1). After each round of needle punching, the weight of the felt was measured. This was used to calculate the PLA loss percentage and HF/PLA ratio. Figure 4-1 shows the PLA loss percentage vs needle punching round. It can be seen that for about 6 to 7 rounds of needle punching, the PLA loss appears to stabilize at around 20%. However, some outliers do exist in the graph. Samples S1 and S6 were very loosely formed during carding process and the loose fiber compactness led to an increased loss of PLA powder. Sample S2 seems to be consistent with other samples up to round 5, after which it was flipped over, which led to a greater loss of PLA.

It was concluded that for a 50/50 fiber PLA mix, the PLA loss stabilizes after approximately 7 rounds at nearly 20%. The process adopted for final sample preparation is shown in Appendix A-1. Figure 4-2 shows the layers of the final composite sample due to folding and PLA addition. It was decided to use 8 rounds of needle punching and adding 20% extra PLA to achieve the desired ratios.

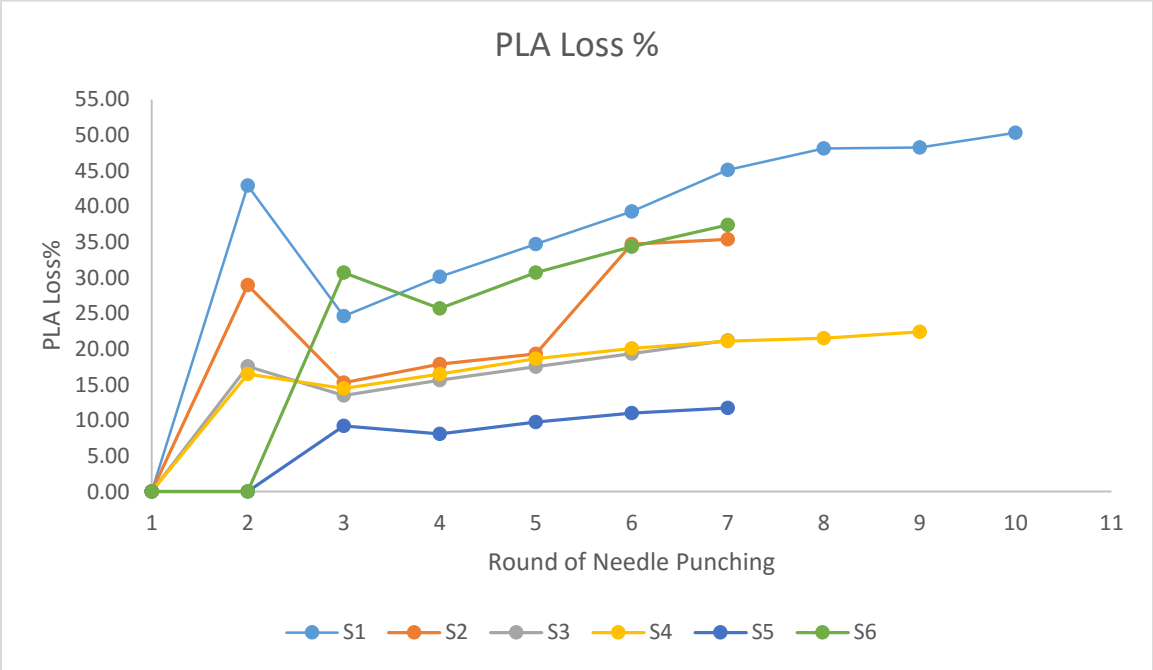

Figure 4-1 Felt Fabrication: PLA Loss % vs Needle Punching Round

Figure 4-2 Figure 4 1 Cut-away of layered composite felt

The blue dotted texture represents PLA powder. The diagram only represents the layered structure after needle punching and not the penetration of the PLA powder due to needle punching.

4.2 Compression Molding Parameters Results

The samples were visually tested to check for the presence of PLA powder throughout the thickness and also relative strength. The samples were freeze-fractured, by dipping into liquid Nitrogen for about 45 seconds and snapping with pliers. The results showed that the lowest processing parameters of 180˚C for 100 seconds had the most residual PLA powder, indicating poor melting. The bottom few layers of the samples were still highly fibrous. The best results for each sample were obtained for the highest parameters of 190˚C for 120 seconds (Figure). Zero to negligible PLA powder was observed for most samples processed at this condition and they also showed better strength. This indicated complete PLA melting. The bottom layer was still fibrous, but to a very minimal depth. It was speculated that the bottom layer would be fibrous, due to the addition of PLA only from the top, which coincides with the observations.

Figure 4-3 (a) shows a SEM image of the total thickness of a sample. The images of top, middle and bottom sections of the composite are also shown. The images showed the manner of PLA distribution throughout the thickness. These samples were hot pressed at 190˚C for 120 seconds and show adequate melting and dispersion of the matrix. The samples at lower compression molding conditions were too fibrous and did not produce appropriate SEM results.

It was concluded to use the conditions – temperature of 190˚C, pressure of 5 bar, and time of 120 seconds for the final sample preparation.

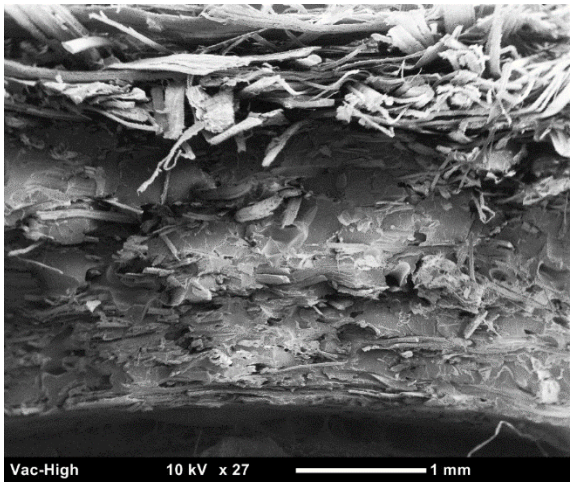

(a) Full thickness (image is flipped)

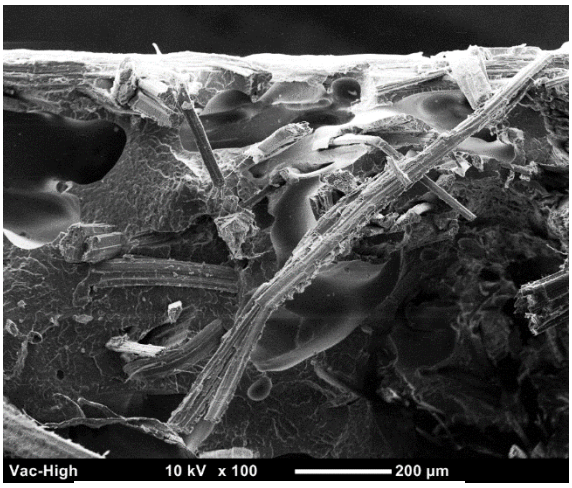

(b) Near top surface

(c) Near mid thickness

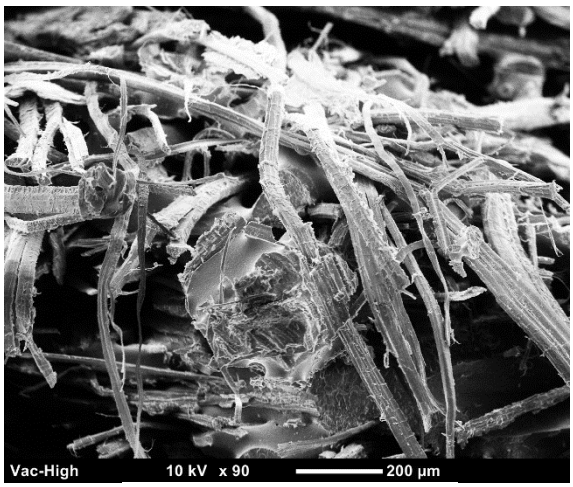

(d) Near bottom surface

Figure 4-3 SEM images showing PLA and fiber adhesion from top to bottom

4.3 Tensile Properties

Each sample had 3 replicates and the mean and range values for the tensile testing results were recorded. The samples were named T1, T2, T3, T4, T5 and T6 and Table 4-1 shows the results of the testing. The numbers in the brackets denote the range. Appendix A-2 gives the details of the individual sample results. It should be noted that Sample 4 had only two replicates due to sample panel size constraints. Specimen 1T1 was an outlier in the Sample 1 batch, with a tensile strength of only 4.22 MPa. This is believed to be because the specimen was taken from the edge of the sample panel, where PLA dispersion was less uniform.

The average tensile strength for 55% fiber loading was 14.76 MPa, for 50% fiber loading was 18.55 MPa and for 35% fiber loading was 17.5 MPa. The average values for the elastic modulus were 1048.67 MPa for 55% loading, 1175 MPa for 50% loading, and 863 MPa for 35% loading. Figure 4-4, Figure 4-5 and Figure 4-6 show the variation of tensile strength, modulus, and elongation at yield with fiber loading, respectively. These results are comparable to the tensile strengths of KP composites and exceed those of BP and RP composites obtained by Chen Y (2005), where KP (kenaf/PP) had the highest tensile strength of 17.039 MPa and a modulus of 327.237 MPa [36]. However, N. Martin et al. (2016) reported a maximum tensile strength of 93 MPa and modulus of 9569 MPa for paper processed flax/PP mats, with MAPP as a coupling agent, at 40% fiber loading [42]. This difference represents the poor adhesion between the hydrophilic fibers and hydrophobic polymers without suitable modification of the fibers. This also shows from the fact that the composite strength was reduced as compared to strength of PLA and hemp fiber individually. The poor wettability of hemp by the PLA, resulted in poor

adhesion, leading to easy fiber pullout instead of the fiber bearing the load (Figure 4-7), hence reducing the available strength.

For most cases, the tensile strength at yield was the same as ultimate tensile strength (Table 4-1) and the % Elongation at yield did not vary much with a mean of 2.45% and standard deviation of 0.25%. This shows the brittle or non-ductile nature of the composite. The elongation at break of most samples showed very high values, which was because of fiber entanglement (Figure 4-7), which supported negligible tensile loading after yield, as can be seen in Figure 4-8.

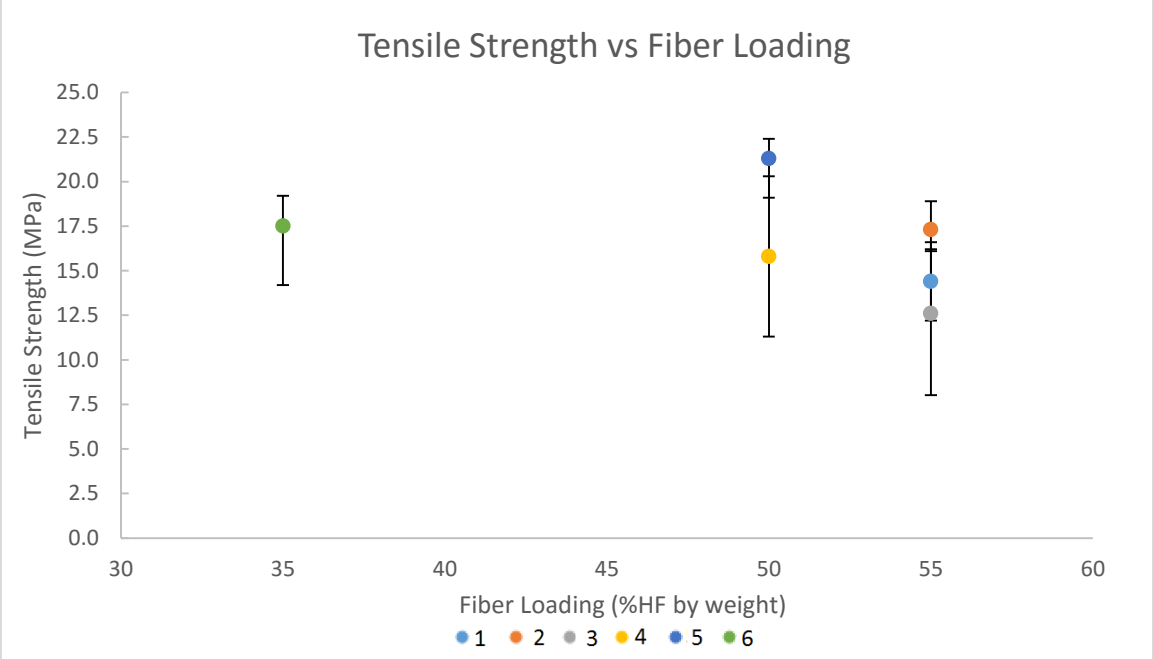

Figure 4-4 Tensile strength vs. fiber loading

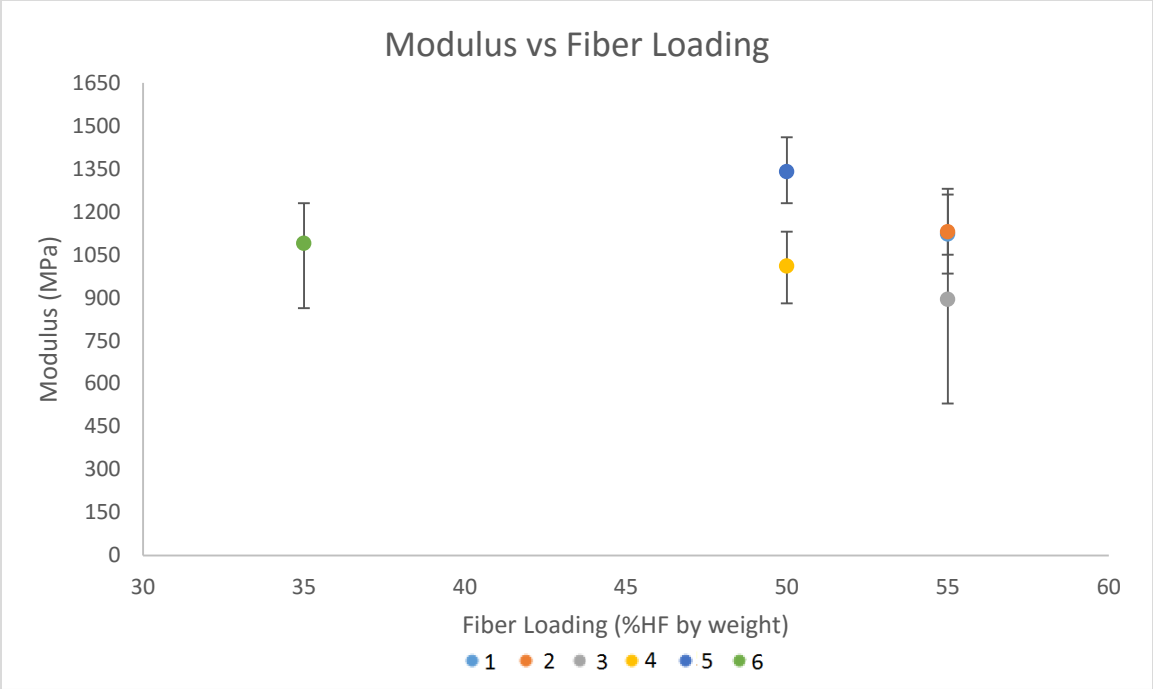

Figure 4-5 Elastic modulus vs. fiber loading %

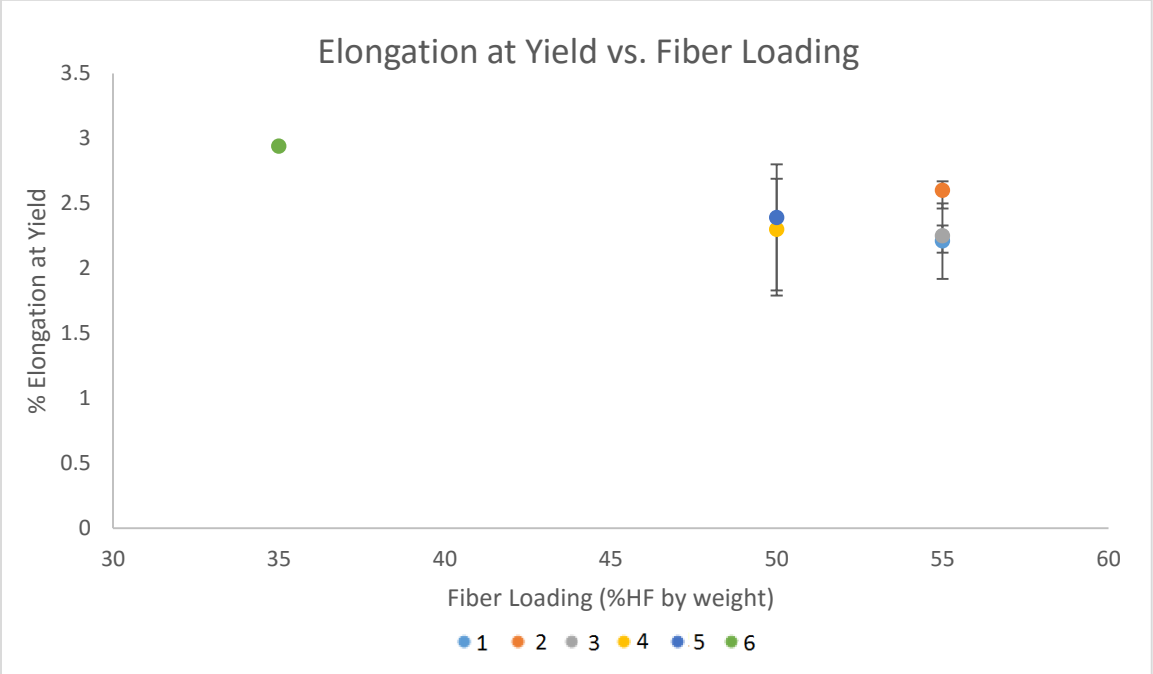

Figure 4-6 Elongation at yield vs. Fiber loading

Table 4-1 Tensile testing results

Sample	Fiber loading	Tensile Strength	Tensile Strength	% Elongation at	Tensile Strength	% Elongation	Modulus	Modulus (Sec 1 %)	Width	Thickness
	%	(MPa)	at Yield (MPa)	Yield (%)	at Break (MPa)	at Break(%)	(MPa)	(MPa)	(mm)	(mm)
T1	55	14.4(4.4)	14.4(4.4)	2.21(0.58)	0.0166(0.009)	39(6.2)	1122(276)	927(136)	25.4	3.665(0.23)
T2	55	17.3(2.8)	17.3(2.8)	2.6(0.21)	0.0379(0.0199)	33.5(2.1)	1130(230)	980(182)	25.4	3.73(0.27)
T3	55	12.6(8.19)	12.6(8.19)	2.25(0.21)	0.232(0.132)	17.9(6.4)	894(589)	769(496)	25.4	3.56(0.17)
T4	50	15.8(9)	15.8(9)	2.3(1.01)	0.139(0.064)	17.2(1.3)	1010(250)	921(293)	25.4	3.4(0.01)
T5	50	21.3(3.3)	21.3(3.3)	2.39(0.86)	10.8(16.542)	5.79(8.72)	1340(230)	1130(130)	25.4	3.48(0.04)
T6	35	17.5(5)	14.2(0)	2.94(0)	17.4(5.2)	2.69(0.59)	1090(367)	863(267)	25.4	4.35(0.75)

Figure 4-7 Tensile testing - fiber entanglement after yielding

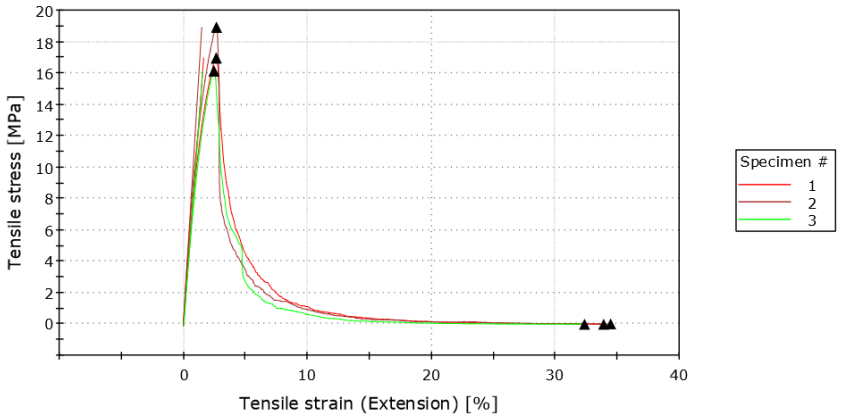

	Tensile Strength [MPa]	Tensile Strength at Yield [MPa]	% Elongation at Yield [%]	Tensile Strength at Break [MPa]	% Elongation at Break [%]	Modulus [MPa]	Modulus (Secant 1 %) [MPa]	Width [mm]	Thickness [mm]
1	17.0	17.0	2.66	0.0318	33.8	1,050	963	25.4	3.83
2	18.9	18.9	2.67	0.0509	34.4	1,280	1,080	25.4	3.81
3	16.1	16.1	2.46	0.0310	32.3	1,050	898	25.4	3.56
Mean	17.3	17.3	2.60	0.0379	33.5	1,130	980	25.4	3.73
S.D.	1.424	1.424	0.117	0.011	1.094	131	92.113	0.000	0.150

Figure 4-8 Stress - strain graph of Sample 2 specimens

A graphical comparison between the tensile strengths of different fiber loading levels and samples cited from previous works is shown in Figure 4-9. The corresponding comparison of the elastic modulus is shown in Figure 4-10. Here, T1 represents a kenaf/PP composite [40], T2 represents a ramie/PP composite [41], T3 represents a MAPP modified flax/PP composite [42] and T4 represents a glass fiber/Polyester composite [43]. It can be seen from both figures that the 50% fiber loading, with a tensile strength and modulus of 18.55MPa and 1175MPa, respectively, performs slightly better than the other loading levels. All samples perform at par or better than other non-modified natural fiber composites. The kenaf/PP composite had better properties than the ramie/PP composite, with a strength and modulus of 14MPa and 1563MPa, respectively. The flax/PP composite with MAPP modification outperformed every other composite, including the glass fiber reinforced polyester composite. This can be attributed to the excellent adhesion between the fiber and matrix through the coupling agent.

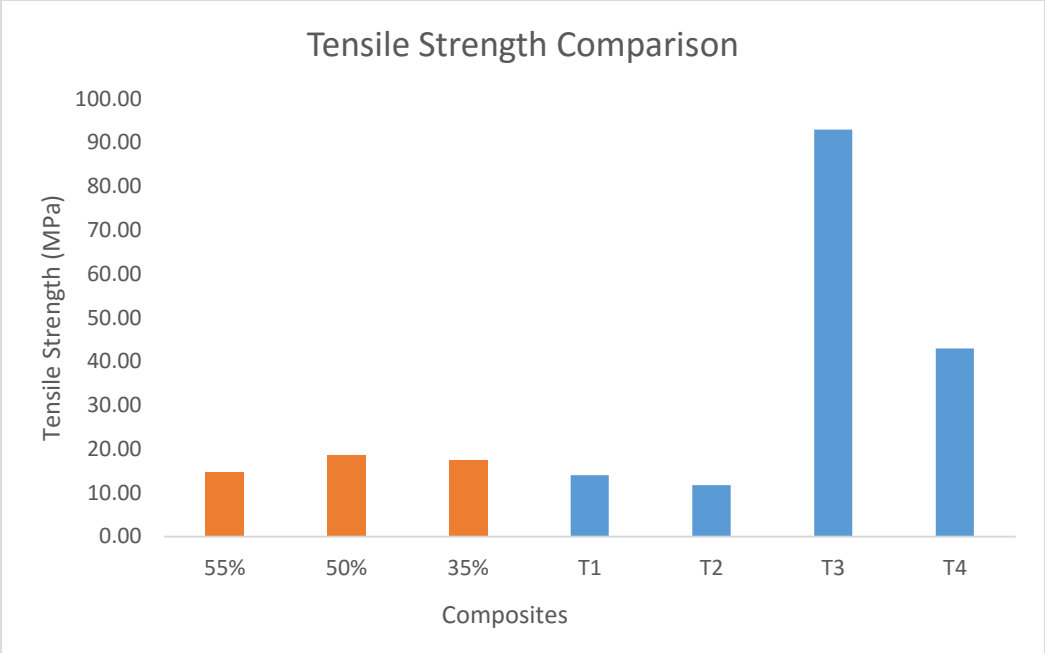

Figure 4-9 Comparison of tensile strengths of various NFCs

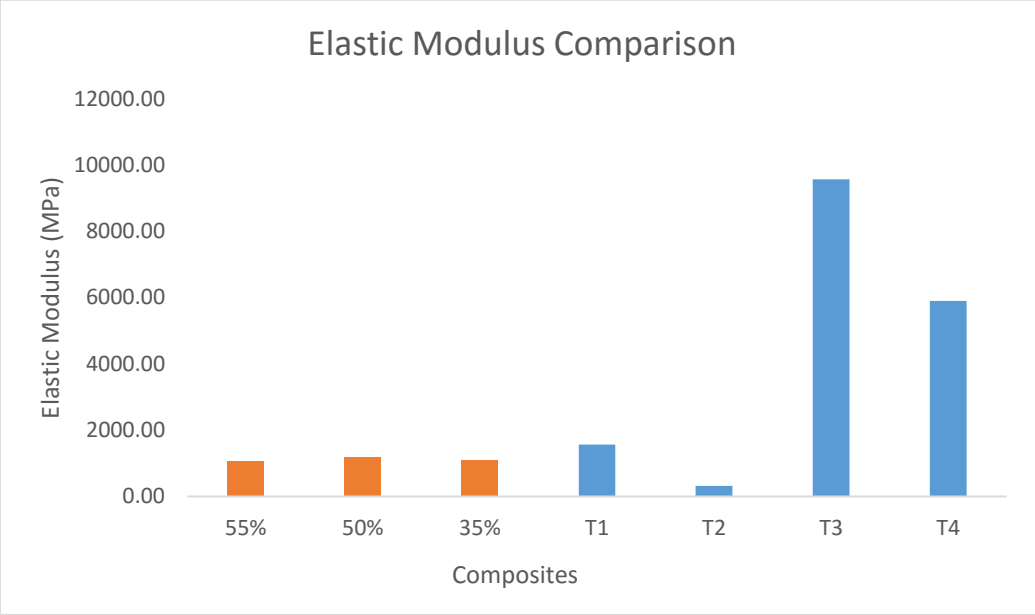

Figure 4-10 Comparison of tensile moduli of various NFCs

4.4 Impact Properties

The impact properties were averaged over two trials for each sample and the results are shown in Table 4-2. The average impact energy for 55% fiber loading was found to be 1.774 J/cm^2, for 50% it was found to be 1.749 J/cm^2 and for 35% it was found to be 1.618 J/cm^2. It shows that near 50% fiber loading has the optimum breaking energy. These values show reduction in impact strength from that of pure PLA (2.05 J/cm^2): 13.45% reduction for 55% loading, 14.68% reduction for 50% loading and 21.07% reduction for 35% loading. This is attributed to the fiber-polymer adhesion characteristics. This can be seen from the impact energies recorded in a work by Pickering et al., where a coupling agent (MAPP) is used in hemp/PP composites, showing an impact strength of 21 J/cm^2 [47]. It can be seen that most samples had a partial or hinge breaks (Figure 4-13). This is because of the dense entanglement of the fibers throughout the thickness of the composite and the toughness of those fibers. Only sample 6 (35% fiber loading) specimens had complete breaks. The values obtained were comparable to other non-modified natural fiber composites. They exceeded the impact strengths of EFB/Jute/Epoxy sandwich components [45] and compare closely to kenaf/PP and wood/PP composites [46] [47]. Figure 4-11 shows the comparison of impact energies between different non modified natural fiber composites. I1 represents a bamboo/PLA composite [44], I2 represents a kenaf/PP composite [46] and I3 represents a wood/PP composite [47]. The impact strengths of the hemp/PLA composites produced here remain lower than kenaf/PP and wood/PP composites, but outperform bamboo fiber reinforced polypropylene. The impact strengths however remain significantly low when compared to modified fiber reinforced composites as can be seen in Figure 4-12.

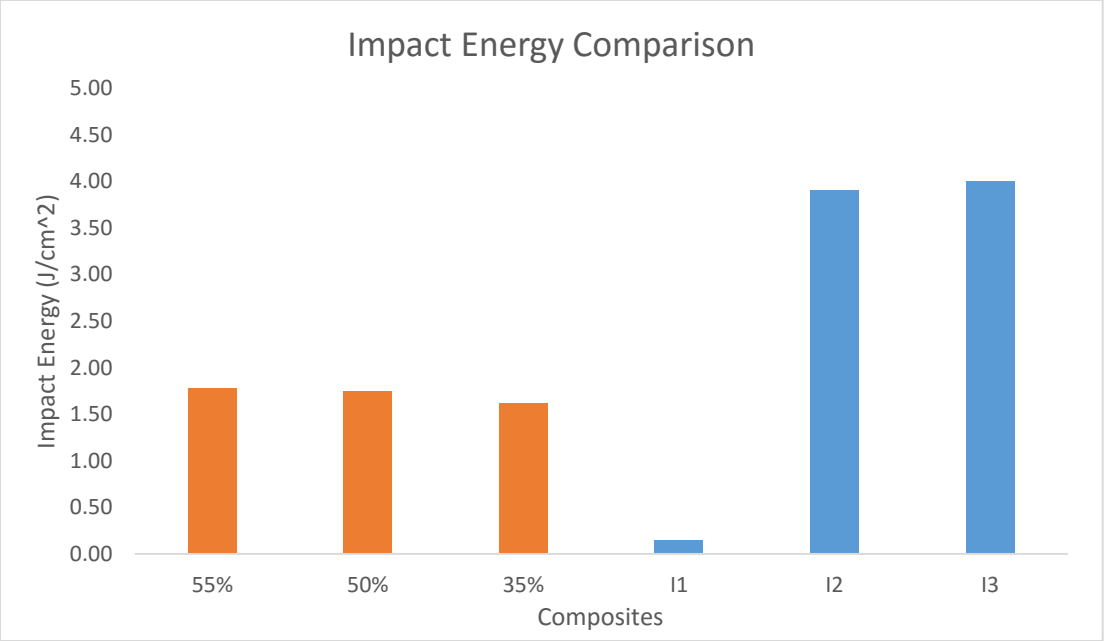

Figure 4-11 Comparison of impact energies of non-modified natural fiber composites

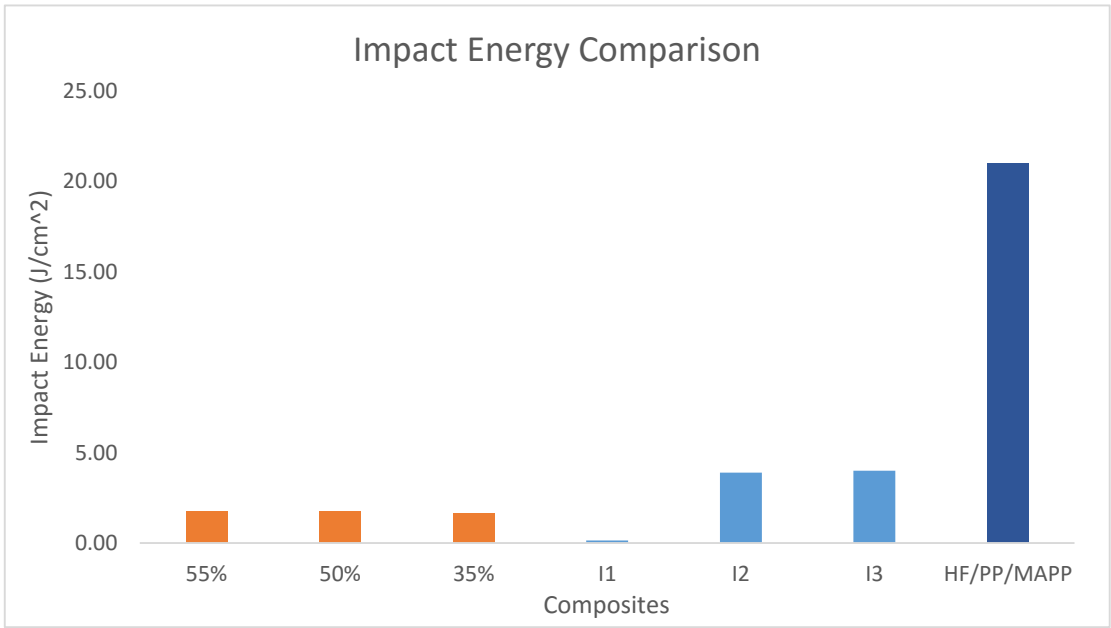

Figure 4-12 Comparison of impact energies of with a MAPP modified NFC

Table 4-2 Izod impact test results

Sample	Specimen 1 BE (J/cm^2)	Specimen 2 BE (J/cm^2)	Ave BE BE (J/cm^2)	Specimen 2 Angle	Specimen 1 Angle	Average Angle
1	1.940	2.276	2.108	106	100	103
2	1.722	1.777	1.750	110	109	110
3	1.354	1.577	1.466	117	113	115
4	1.767	NA	1.767	109	NA	109
5	1.694	1.768	1.731	112	110	111
6	1.585	1.651	1.618	109	110	110

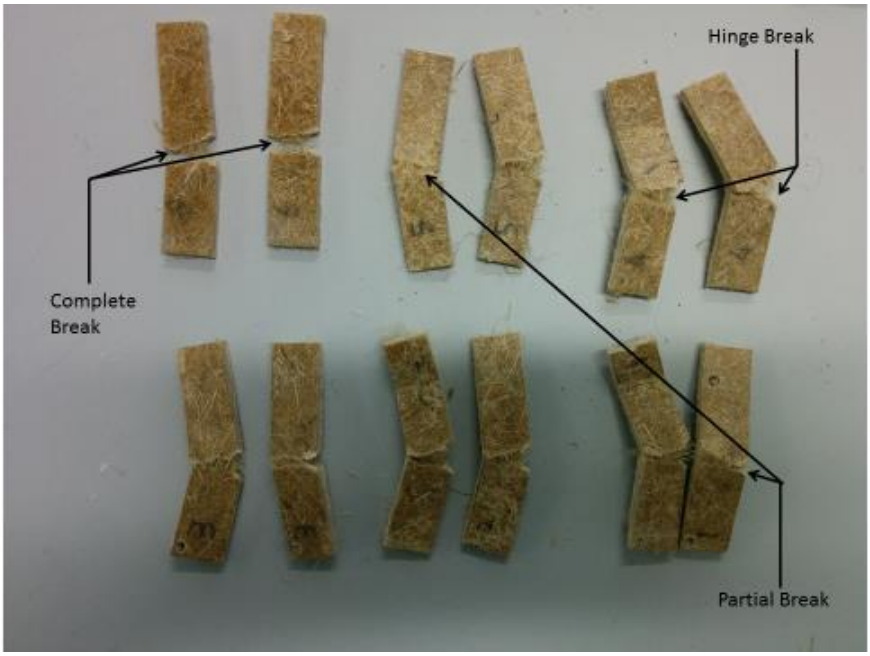

Figure 4-13 Impact testing results showing type of break in each specimen

Partial Break - Thick portion unbroken
Hinge Break – Fibrous portion unbroken
Complete Break – Specimen separates into two parts

4.5 Acoustic Properties

Absorption Coefficient

Since the top and bottom surfaces of the composites were different, measurements were made with both sides facing the sound source. Figure 4-16 shows the absorption coefficient values for fibrous surface facing the sound source (straight) and Figure 4-15 represents the reverse case, at increasing frequencies.

Sample 2 and Sample 5 showed the highest absorption coefficient of around 0.56 at nearly 6.4 KHz (Figure 4-18), for straight measurements. It can be seen that in the low frequency range (0-1.6KHz), the absorption coefficients were approximately under 0.12 (Figure 4-17). In the higher frequency range (>5 KHz) most composites showed coefficients between 0.3-0.5. There was a sharp increase in the absorption for most samples between the frequency range 4 KHz – 5 KHz (Figure 4-18).

For the reversed samples, the absorption coefficients at low frequency (up to 1.6 KHz) the coefficients remained under approximately 0.22 (Figure 4-19). At higher frequencies (around 5-6 KHz) the sample showed coefficients ranging from 0.16 to 0.36, besides Sample 2 which had a peak of 0.72 (Figure 4-20). All the samples had peaks at varying frequencies, between 3.6 KHz and 6.2 KHz. Besides Sample 2, which shows a relatively high absorption coefficient, the highest peak was at 0.55 for Sample 5.

It appeared that at low frequencies, the reverse samples (plastic surface facing sound source) had better absorption characteristics. At higher frequencies (>1.6 KHz) the straight samples (fibrous surface facing the sound source) performed better.

In relation to fiber loading, it was seen that the 50% fiber loaded composites (Samples 4 and 5) had the best absorption characteristics. The 35% fiber loading had the lowest overall values, which was expected due to higher polymer content.

Overall, the absorption coefficients concurred with the range of previously documented works. Chen et al. (2010) reported absorption coefficients for flax felts and flax/PP panels. The panels had a coefficient <0.3 for all ranges, while the felts reached 0.6 at nearly 6 KHz [52]. The results for composite panels obtained here measure closer to the felts, while retaining their mechanical strength. Koenig and Mueller tested hemp/PP composites and recorded the highest absorption coefficient of 0.4 at 6 KHz [53], which also compares closely to the results observed here.

Figure 4-14 shows the comparison of the absorption coefficients of the different fiber loading levels with previously cited data. C1 refers to a kenaf/PP composite fabricated by Chen et al. (2012) [40], C2 is a PP/Hemp R4 sample produced by Koenig and Mueller [53] and C3 is a flax/PP panel fabricated by Chen et al. (2010) [52]. We can see from the graph that the samples produced here faired above the hemp/PP and flax/PP composites, but did not perform as good as the kenaf/PP composites. The reason cited for the high coefficients for the kenaf/PP composites is the low temperature and short time allowed for compression molding, which left the panels porous and unsolidified. Hence they resembled the properties of felts over panels, which can be seen in their mechanical strengths. Among the various fiber loadings, the 50% fiber loaded samples seem to have optimum performance, followed closely by 55% fiber

loading, with 35% fiber loading having the worst performance. This is understandable as fiber is the better sound absorbing component in the composite and higher levels should yield better absorption.

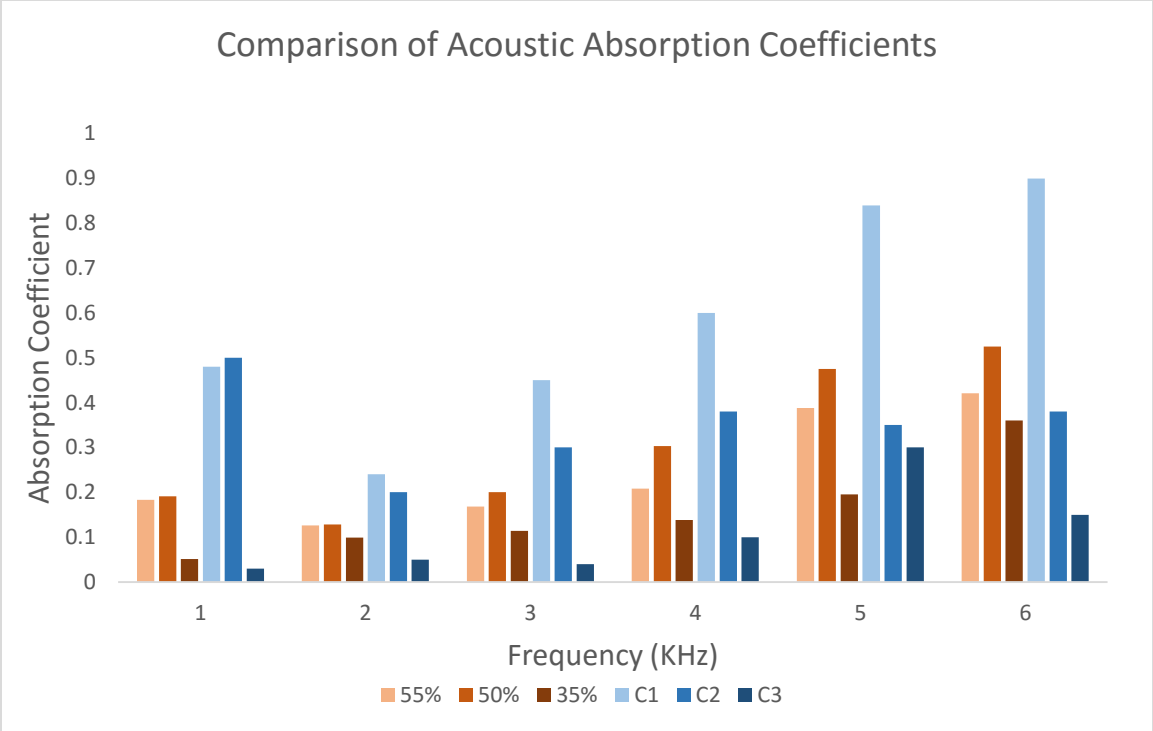

Figure 4-14 Comparison of acoustic absorption coefficients of various NFCs

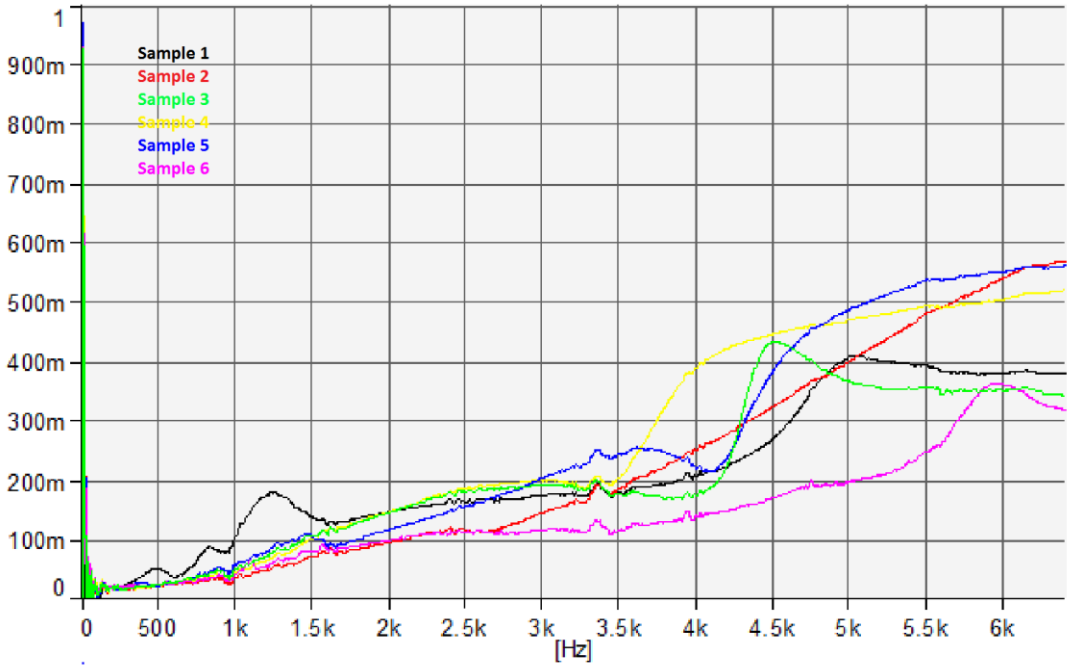

Figure 4-15 Acoustic absorption: fibrous surface facing sound source

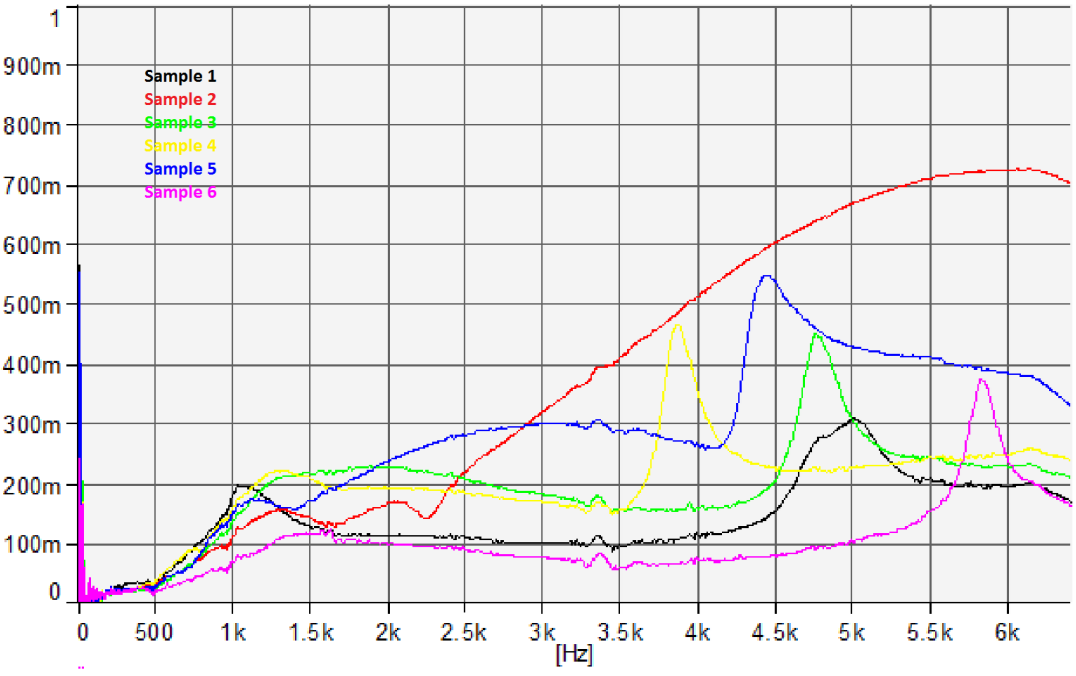

Figure 4-16 Acoustic absorption: plastic surface facing sound source (reverse)

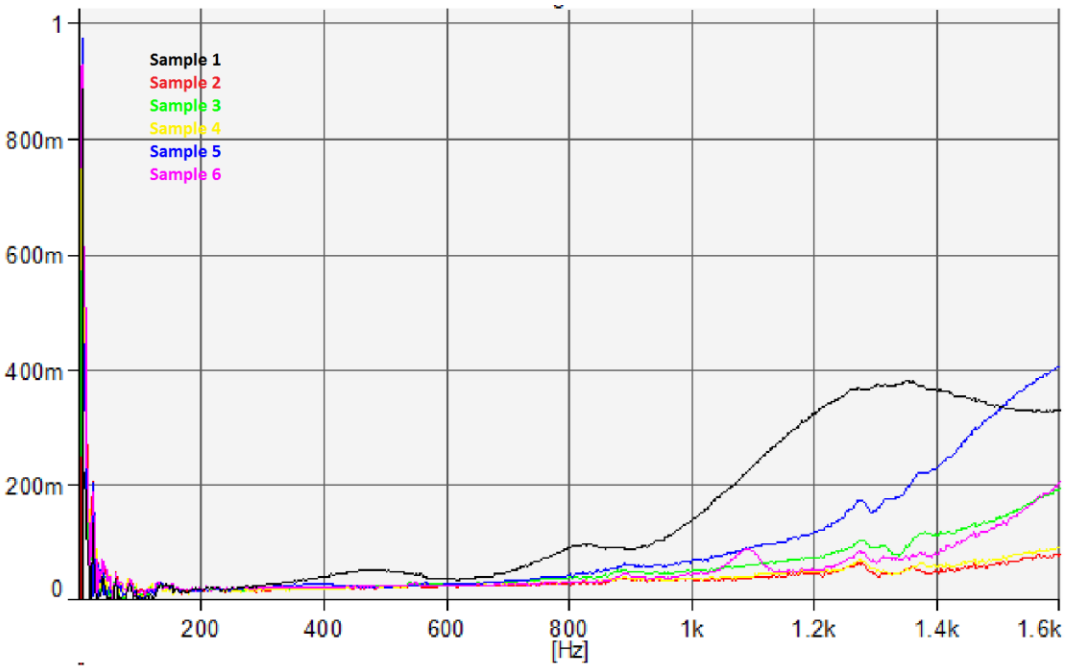

Figure 4-17 Acoustic absorption at low frequency: fibrous surface

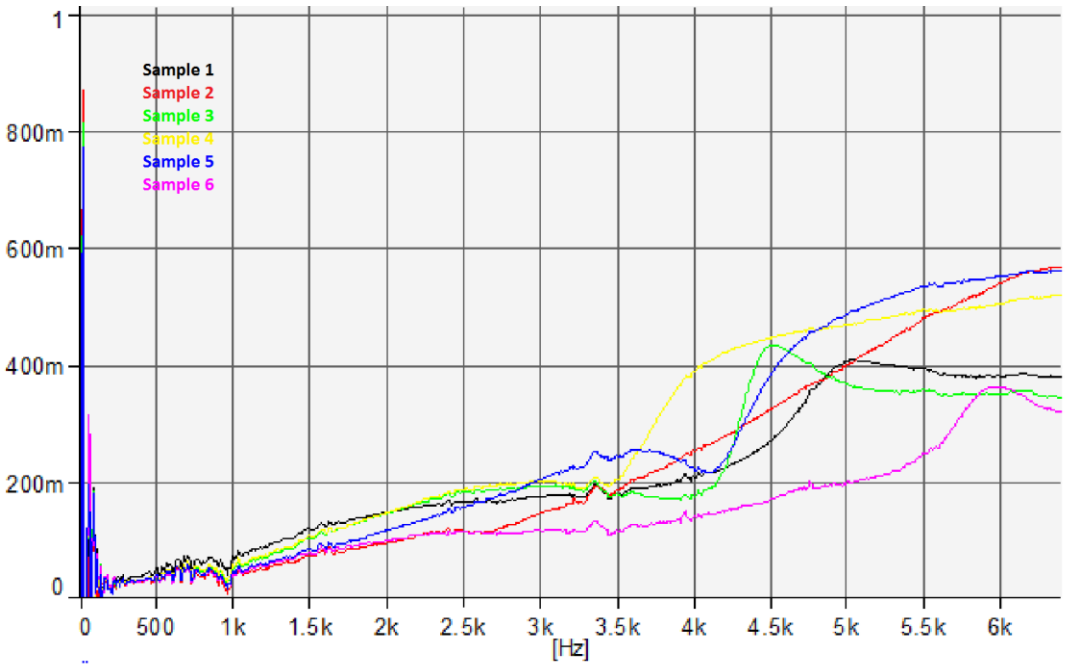

Figure 4-18 Acoustic absorption at high frequencies: fibrous surface

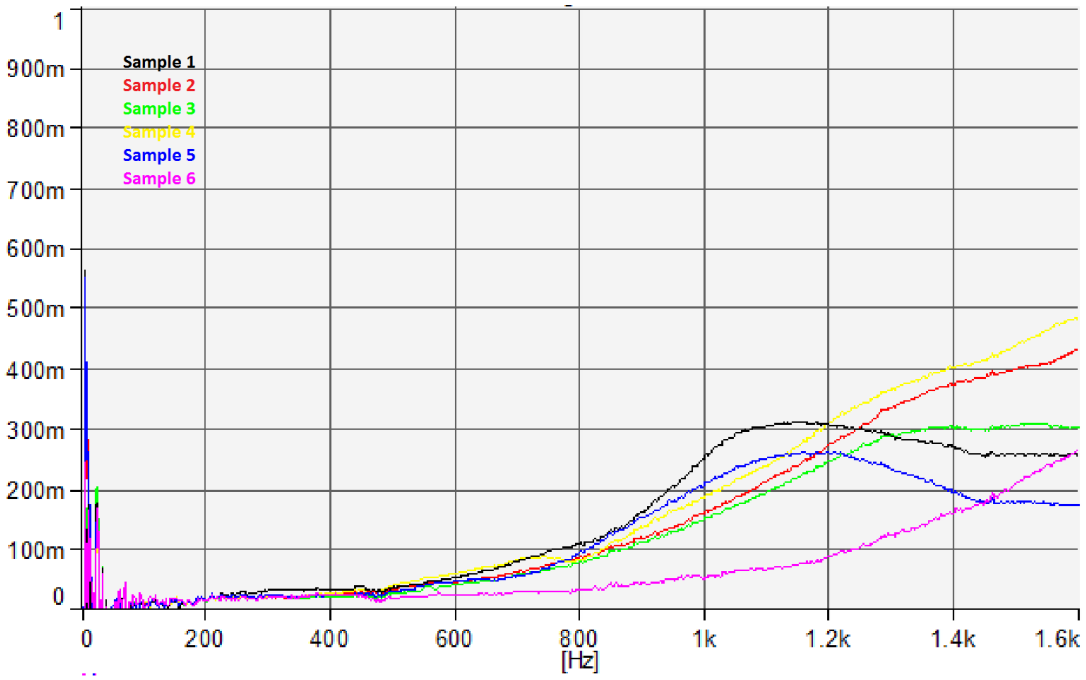

Figure 4-19 Acoustic absorption at low frequencies: reversed samples

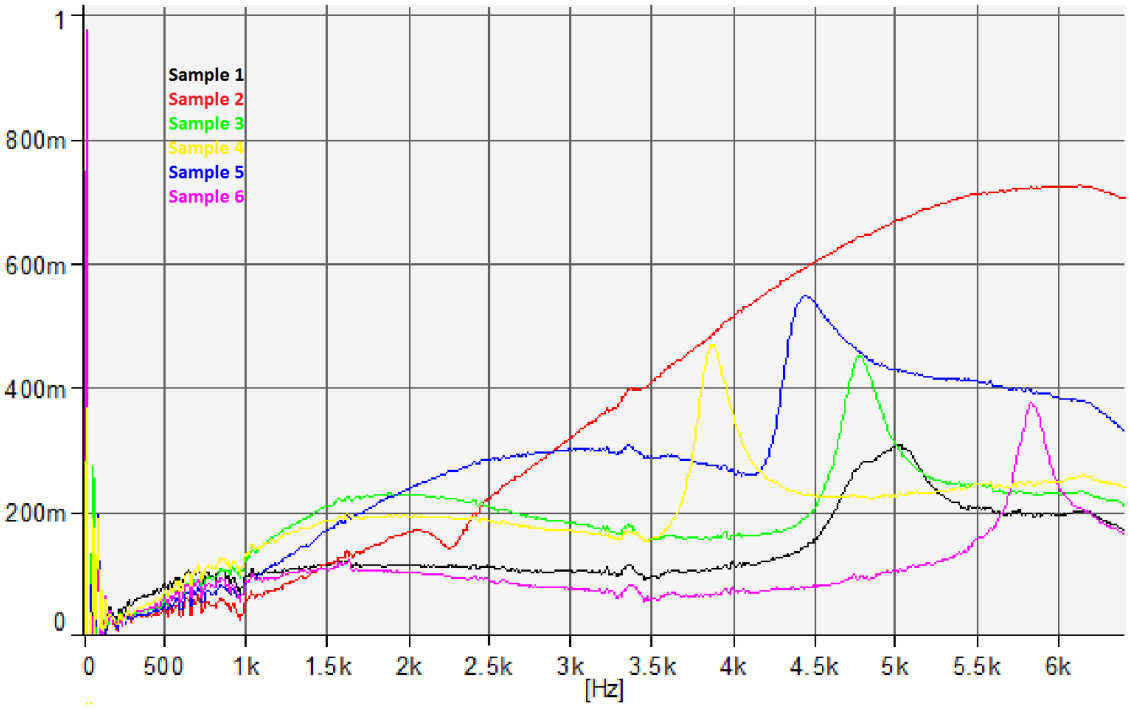

Figure 4-20 Acoustic absorption at high frequencies: reversed samples

4.6 Dynamic Mechanical Analysis Results

Dynamic mechanical analysis was carried out on the composite samples to test for the mechanical modulus and glass transition temperatures. Figure 4-21, representing Sample 4 (50% fiber loading), is an example of the DMA analysis plot. The glass transition temperatures (Tg) were found to be 68.97˚C, 62.19˚C and 59.15˚C for 55%, 50% and 35% fiber loading respectively, demonstrating a decrease in Tg with increasing fiber loading, which shown by the peak of tan δ. This can be due to the higher Tg of lignin (110-150˚C) [56] as compared to PLA (~60˚C). Higher fiber loading leads to a higher proportion of lignin in the composite, which increases the Tg. Overall, the Tg values are closer to the PLA glass transition range.

The storage modulus and the damping (tan δ) values for all the samples were recorded and averaged according to their fiber loading levels (Table 4-3). Tan δ represents the ratio of the loss to storage modulus and is a measure of the energy dissipation of a material. The higher the value of tan δ, the better will be the energy absorption. It can be seen that the 50% fiber loading

Table 4-3 DMA testing results

Fiber Loading %	Sample	Tg (˚C)	Storage Modulus(MPa)	Tan δ
55	**1**	65.80	1750.00	0.48
	2	63.30	800.00	0.22
	3	77.80	680.00	0.23
	Ave	**68.97**	**1076.67**	**0.31**
	Range	**14.50**	**1070.00**	**0.26**
50	**4**	64.11	1325.00	0.63
	5	60.27	950.00	0.58
	Ave	**62.19**	**1137.50**	**0.61**
	Range	**3.84**	**375.00**	**0.05**
35	**6**	59.15	210.00	0.38
	Ave	**59.15**	**210.00**	**0.38**
	Range	**-**	**-**	**-**

had the greatest storage modulus at 1137.5 MPa and damping coefficient at 0.61. The 35% fiber loaded sample had the least value for storage modulus and a low tan δ value, indicating low energy absorption characteristics.

Figure 4-21 shows peaks for tan δ at 64˚C, 95 ˚C and 110 ˚C. The second peak at 95 is assumed to be due to the breakdown of the crystalline PLA and the third peak is assumed to refer to the breakdown of lignin in the fibers. This trend is common throughout most of the samples (Appendix A-3).

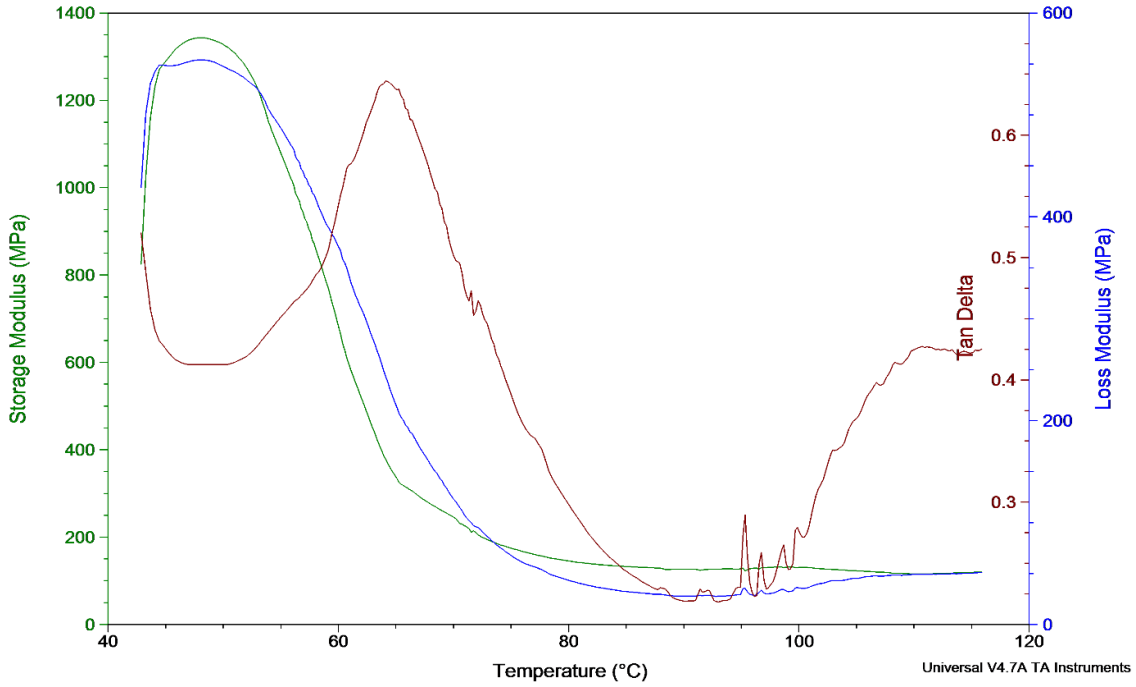

Figure 4-21 DMA analysis plot for Sample 4, showing storage modulus, loss modulus and damping coefficient

4.7 Thermal Properties

The thermal conductivity values were calculated for the different fiber loading levels at varying temperatures and the results are shown in Figure 4-22. The temperature does not seem to have a major effect on the conductivity values. The 50% fiber loaded composites recorded the lowest thermal conductivities, followed by the 55% loading level composites. The composites with 35% fiber loading had the highest conductivity. The average values of thermal conductivities based on fiber loading were found to be 0.109 W/m-k, 0.083 W/m-K and 0.129 W/m-K for 55%, 50% and 35% loading levels, respectively. The low value of 35% loading can be understood from the fact that the fibers are porous and contain trapped air, with a k value of 0.024 W/m-K, which reduces the heat conduction through the material. Therefore a lower loading level would result in a higher conductivity.

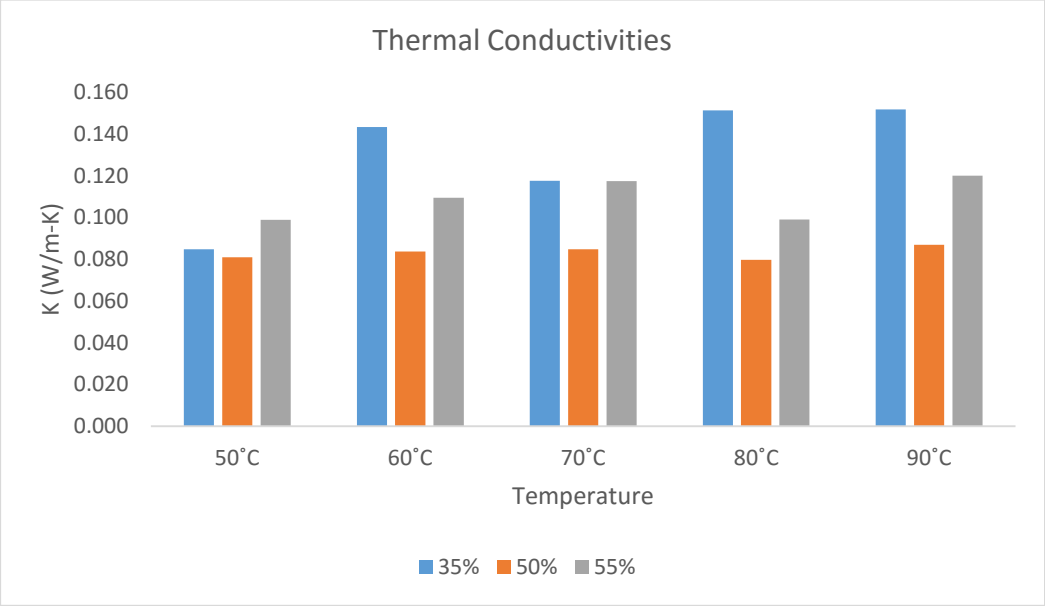

Figure 4-22 Thermal conductivities of different fiber loadings at varying temperatures

The conductivity values obtained show that the composites are good thermal insulators with characteristics resembling their counterparts in automotive insulation applications. The conductivities are lower than most automotive polymeric materials as discussed previously [51]. Previous works on hemp/polymer composites showed conductivities of 0.20 W/m-K and 0.25 W/m-K, at different fiber loading levels[50], while plastics range from 0.17 – 0.50 W/m-K [51]. Table 4-4 shows the thermal conductivity results for each sample.

Table 4-4 Thermal conductivity experimental results

Sample	Trial	K (W/m-K) @ Temp					Average
		50C	60C	70C	80C	90C	
1	1	0.1169	0.0966	0.1091	0.1034	0.1181	0.1088
	2	0.0622	0.0975	0.1175	0.1050	0.1250	0.1014
	3	0.1023	0.2230	0.1599	0.1568	0.2089	0.1702
	Ave	**0.0938**	**0.1390**	**0.1288**	**0.1217**	**0.1506**	**0.1268**
	Range	**0.0547**	**0.1264**	**0.0509**	**0.0534**	**0.0908**	**0.0641**
2	1	0.1198	0.1364	0.1532	0.1330	0.1461	0.1377
	2	0.0727	0.0539	0.1210	0.0602	0.0954	0.0807
	3	0.0626	0.0504	0.0661	0.0597	0.0705	0.0619
	Ave	**0.0850**	**0.0802**	**0.1134**	**0.0843**	**0.1040**	**0.0934**
	Range	**0.0572**	**0.0860**	**0.0871**	**0.0733**	**0.0755**	**0.0758**
3	1	0.1437	0.1121	0.1154	0.1031	0.1207	0.1190
	2	0.1082	0.1400	0.1101	0.0933	0.1085	0.1120
	3	0.1008	0.0749	0.1043	0.0760	0.0871	0.0886
	Ave	**0.1176**	**0.1090**	**0.1099**	**0.0908**	**0.1054**	**0.1065**
	Range	**0.0429**	**0.0651**	**0.0112**	**0.0271**	**0.0336**	**0.0304**
4	1	0.0753	0.0878	0.0775	0.0912	0.1278	0.0919
	2	0.0693	0.0826	0.0608	0.0510	0.0475	0.0622
	3	0.0712	0.0825	0.0939	0.0849	0.0984	0.0862
	Ave	**0.0719**	**0.0843**	**0.0774**	**0.0757**	**0.0912**	**0.0801**
	Range	**0.0060**	**0.0053**	**0.0331**	**0.0402**	**0.0803**	**0.0297**
5	1	0.1047	0.1129	0.1071	0.1007	0.0838	0.1018
	2	0.0752	0.0530	0.0771	0.0663	0.0816	0.0707
	3	-	-	-	-	-	-
	Ave	**0.0899**	**0.0830**	**0.0921**	**0.0835**	**0.0827**	**0.0863**
	Range	**0.0295**	**1.1083**	**0.0300**	**0.0344**	**0.0022**	**0.0024**
6	1	0.1183	0.1330	0.1196	0.1504	0.1734	0.1389
	2	0.0511	0.1537	0.1154	0.1522	0.1299	0.1205
	3	-	-	-	-	-	-
	Ave	**0.0847**	**0.1433**	**0.1175**	**0.1513**	**0.1516**	**0.1297**
	Range	**0.0419**	**0.0129**	**0.0026**	**0.0011**	**0.0271**	**0.0115**

Chapter 5 Conclusions and Future Work

5.1 Summary and Conclusions

A novel method of making non-woven composites, utilizing the powder form of the polymer, was tested and the composite material's mechanical properties were characterized. The PLA loss through the process was found to be near 20% by weight, which could be recovered and recycled. The densities of the composites were uniform throughout, at an average of 0.62 g/cm^3. Sample 6 had a higher density of 0.84 g/cm^3, because of a higher PLA content.

Table 5-1 tabulates all of the recorded results. The composite showed mechanical strengths in the range of previously cited non-modified natural fiber composites. In most cases, the tensile strength and modulus exceeded other NFCs, with an average value of 16.94 +/- 3.78 MPa and 1104.6 +/- 126.3 MPa, respectively. The impact strengths faired equally well as other NFCs, with an average value of 1.71 +/- 0.16 J/cm^2. The composites formed showed brittle behavior with an average elongation at break (or yield) of 2.55 +/- 0.6%. The impact and tensile tests showed the low shattering properties of the material due to fiber entanglement. This is a useful safety feature for automobile and transport applications. The strengths were reduced compared to the individual components, due to poor fiber - polymer adhesion. The optimum fiber loading was found to be near 50%, for all mechanical properties. Table 5-1 was used to find the specific strengths of the composites. The maximum values of specific tensile strength and modulus were 26.65 MPa and 1688.2 MPa, respectively for 50% fiber loading. These are acceptable values, but could be improved by the use of a coupling agent.

The finished composite had two different finished surfaces – fibrous and plastic. This allowed different orientations to have different acoustic absorption properties at varying frequency ranges. The plastic surface had a greater coefficient of absorption at lower frequencies (<1.2 KHz) and the fibrous surface had better absorption in the higher frequency range (1.2 – 6.4 KHz). The average absorption coefficient of the samples was found to be 0.15 +/- 0.1 for low frequencies (1.2 KHz) and 0.44 +/- 0.17 for higher frequencies (6 KHz). The 50% fiber loaded samples showed the best characteristics with an absorption coefficient of 0.19 in the low and 0.53 in the high frequency ranges.

The composites showed good thermal resistance with an average thermal conductivity of 0.107 +/- 0.026 W/m-K. The least thermal conductivity was observed for 50% samples at 0.083 +/- 0.006 W/m-K. The dynamic mechanical analysis showed that the 50% fiber loaded samples had the greatest storage modulus at 1137.5 +/- 375 MPa with a glass transition temperature at 62.19˚C. They also showed a high tan δ value indicating good energy dissipation and high energy absorption capabilities.

Fiber Loading	Sample	Density	Tensile Strength	Elastic Modulus	Elongation at Yeild	Elongation at break	Impact Strength	Storage Modulus	Tg	Tan δ	Thermal Conductivity	Acoustic Absorption Coefficient	
(%)	#	(g/cm^3)	(MPa)	(MPa)	(%)	(%)	(J/cm^2)	(MPa)	(˚C)		(W/m-K)	1.2 KHz	6.0KHz
55	**1**	0.692	14.40	1122.0	2.21	39.00	2.11	1750.0	65.80	0.48	0.127	0.17	0.38
	Range	0.164	4.40	276.0	0.58	6.20	0.34	-	-	-	0.064	-	-
	2	0.583	17.30	1130.0	2.60	33.50	1.75	800.0	63.30	0.22	0.093	0.15	0.54
	Range	0.126	2.80	230.0	0.21	2.10	0.05	-	-	-	0.076	-	-
	3	0.666	12.60	894.0	2.25	17.90	1.47	680.0	77.80	0.23	0.107	0.19	0.35
	Range	0.084	8.19	589.0	0.21	6.40	0.22	-	-	-	0.030	-	-
	Ave	**0.647**	**14.77**	**1048.7**	**2.35**	**30.13**	**1.77**	**1076.7**	**68.97**	**0.31**	**0.109**	**0.17**	**0.42**
	Range	**0.026**	**4.70**	**236.0**	**0.39**	**21.10**	**0.64**	**1070.0**	**14.50**	**0.26**	**0.033**	**0.05**	**0.19**
50	**4**	0.696	15.80	1010.0	2.30	17.20	1.77	1325.0	64.11	0.63	0.080	0.21	0.50
	Range	0.193	9.00	250.0	1.01	1.30	0.00	-	-	-	0.030	-	-
	5	0.696	21.30	1340.0	2.39	5.79	1.73	950.0	60.27	0.58	0.086	0.17	0.55
	Range	0.219	3.30	230.0	0.86	8.72	0.07	-	-	-	0.002	-	-
	Ave	**0.696**	**18.55**	**1175.0**	**2.35**	**11.50**	**1.75**	**1137.5**	**62.19**	**0.61**	**0.083**	**0.19**	**0.53**
	Range	**0.000**	**5.50**	**330.0**	**0.09**	**11.41**	**0.04**	**375.0**	**3.84**	**0.05**	**0.006**	**-**	**-**
35	**6**	0.840	17.50	1090.0	2.94	2.69	1.62	210.0	59.15	0.38	0.130	0.09	0.36
	Ave	**0.840**	**17.50**	**1090.0**	**2.94**	**2.69**	**1.62**	**210.0**	**59.15**	**0.38**	**0.130**	**0.09**	**0.36**
	Range	**0.238**	**5.00**	**367.0**	**0.00**	**0.59**	**0.07**	**-**	**-**	**-**	**0.012**	**-**	**-**

Table 5-1 Summary of results

5.2 Recommendations for Future Work

The research conducted here gives the base for further optimization of the fabrication process and material properties. A predictive model for composite behavior and properties can be made to evaluate and plan future work.

For the current samples further testing of various properties remains to be done – moisture absorption, flame retardancy, chemical resistance are yet to be characterized. The samples could also be foamed, to reduce density, and the new material can be tested and compared to the current samples.

A mechanized method could be established for the handling and dispersion of the polymer powder. This would ensure the application of a uniform layer of the polymer over the fiber mat and minimize losses due to human error. Modifying the needle punching machine would allow us to collect the powder under the needling surface. The step by step procedure for powder addition and felt folding/layering could be further optimized and tested for varying densities and thicknesses.

Using a coupling agent or modifying the hemp fibers chemically, biologically or mechanically would improve the hemp/PLA adhesion, leading to greater strengths. Many methods have been researched for hemp fiber modification. These can be adapted for the fabrication process discussed here. Wetted PLA powder (via modification) could be used instead of dry powder, which would have benefits of better adhesion and reduced PLA loss, but could have an effect on PLA penetration through the hemp mat.

Appendix

A-1 FINAL SAMPLE COMPOSITE FELT FABRICATION PROCESS

Sample #				Before Operation			After Operation					
1	Process	#Round	Operation	PLA Added (gms)	Total PLA Added (gms)	Input Weight(gms)	Output Weight(gms)	PLA Lost (gms)	Total PLA lost (gms)	PLA Left (gms)	Ratio(HF/PLA)	PLA Loss %
						100.0						
	Carding	1										
		2										
		3										
		4					67.3					
	Needle Punching	1	Mat from Carding	0.0	0.0	67.8		0	0	0		
		2	Reverse	0.0	0.0	67.8	67.7	0.0	0.0	0.0		
		3	Fold/add PLA half	33.9	33.9	101.6	98.1	3.5	3.5	30.4	2.23	10.19
		4	Reverse	0.0	33.9	98.1	95.8	2.3	5.8	28.1	2.41	16.99
		5	Fold/add PLA half	33.9	67.8	129.7	127.7	2.0	7.8	60.0	1.13	11.44
		6	Go	0.0	67.8	127.7	126.5	1.2	9.0	58.8	1.15	13.21
		7	Go	0.0	67.8	126.5	124.6	1.9	10.9	56.9	1.19	16.01
		8	Go	0.0	67.8	124.6	123.3	1.3	12.2	55.6	1.22	17.93
2	Process	#Round	Operation	PLA Added (gms)	Total PLA Added (gms)	Input Weight(gms)	Output Weight(gms)	PLA Lost (gms)	Total PLA lost (gms)	PLA Left (gms)	Ratio(HF/PLA)	PLA Loss %
						100.0						
	Carding	1										
		2										
		3										
		4					69.0					
	Needle Punching	1	Mat from Carding	0.0	0.0	69.0	68.9	0	0	0		
		2	Reverse	0.0	0.0	69.0	68.8	0.0	0.0	0.0		
		3	Fold/add PLA half	34.4	34.4	103.2	99.1	4.1	4.1	30.3	2.27	11.92
		4	Reverse	0.0	34.4	99.1	95.6	3.5	7.6	26.8	2.57	22.09
		5	Fold/add PLA half	34.4	68.8	130.0	128.2	1.8	9.4	59.4	1.16	13.66
		6	Go	0.0	68.8	128.2	127.3	0.9	10.3	58.5	1.18	14.97
		7	Go	0.0	68.8	127.3	125.8	1.5	11.8	57.0	1.21	17.15
		8	Go	0.0	68.8	125.8	124.7	1.1	12.9	55.9	1.23	18.75
		9	Go	0.0	68.8	124.7	123.7	1.0	13.9	54.9	1.25	20.20
3	Process	#Round	Operation	PLA Added (gms)	Total PLA Added (gms)	Input Weight(gms)	Output Weight(gms)	PLA Lost (gms)	Total PLA lost (gms)	PLA Left (gms)	Ratio(HF/PLA)	PLA Loss %
						100.0						
	Carding	1										
		2										
		3										
		4					65.9					
	Needle Punching	1	Mat from Carding	0.0	0.0	65.9	65.8	0	0	0		
		2	Reverse	0.0	0.0	65.8	65.8	0.0	0.0	0.0		
		3	Fold/add PLA half	32.9	32.9	98.7	95.3	3.4	3.4	29.5	2.23	10.33
		4	Reverse	0.0	32.9	95.3	92.6	2.7	6.1	26.8	2.46	18.54
		5	Fold/add PLA half	32.9	65.8	125.5	123.2	2.3	8.4	57.4	1.15	12.77
		6	Go	0.0	65.8	123.2	121.7	1.5	9.9	55.9	1.18	15.05
		7	Go	0.0	65.8	121.7	120.8	0.9	10.8	55.0	1.20	16.41
		8	Go	0.0	65.8	120.8	120.0	0.8	11.6	54.2	1.21	17.63
		9	Go	0.0	65.8	120.0	119.7	0.3	11.9	53.9	1.22	18.09
4	Process	#Round	Operation	PLA Added (gms)	Total PLA Added (gms)	Input Weight(gms)	Output Weight(gms)	PLA Lost (gms)	Total PLA lost (gms)	PLA Left (gms)	Ratio(HF/PLA)	PLA Loss %
						100.0						
	Carding	1										
		2										
		3										
		4					64.3					
	Needle Punching	1	Mat from Carding	0.0	0.0	64.3	64.3	0	0	0		
		2	Reverse	0.0	0.0	64.3	64.0	0.0	0.0	0.0		
		3	Fold/add PLA half	38.4	38.4	102.4	98.2	4.3	4.3	34.2	1.87	11.07
		4	Reverse	0.0	38.4	98.2	94.5	3.7	7.9	30.5	2.10	20.57
		5	Fold/add PLA half	38.4	76.8	132.9	129.9	3.0	10.9	65.9	0.97	14.19
		6	Go	0.0	76.8	129.9	127.9	2.0	12.9	63.9	1.00	16.80
		7	Go	0.0	76.8	127.9	126.2	1.7	14.6	62.2	1.03	19.01
		8	Go	0.0	76.8	126.2	125.0	1.2	15.8	61.0	1.05	20.57
5	Process	#Round	Operation	PLA Added (gms)	Total PLA Added (gms)	Input Weight(gms)	Output Weight(gms)	PLA Lost (gms)	Total PLA lost (gms)	PLA Left (gms)	Ratio(HF/PLA)	PLA Loss %
						100.0						
	Carding	1										
		2										
		3										
		4					69.2					
	Needle Punching	1	Mat from Carding	0.0	0.0	69.2	69.2	0	0	0		
		2	Reverse	0.0	0.0	69.2	69.2	0.0	0.0	0.0		
		3	Fold/add PLA half	41.5	41.5	110.7	106.0	4.7	4.7	36.8	1.88	11.33
		4	Reverse	0.0	41.5	106.0	101.5	4.5	9.2	32.3	2.14	22.17
		5	Fold/add PLA half	41.5	83.0	143.0	140.3	2.7	11.9	71.1	0.97	14.34
		6	Go	0.0	83.0	140.3	138.5	1.8	13.7	69.3	1.00	16.51
		7	Go	0.0	83.0	138.5	137.0	1.5	15.2	67.8	1.02	18.31
		8	Go	0.0	83.0	137.0	136.2	0.8	16.0	67.0	1.03	19.28
6	Process	#Round	Operation	PLA Added (gms)	Total PLA Added (gms)	Input Weight(gms)	Output Weight(gms)	PLA Lost (gms)	Total PLA lost (gms)	PLA Left (gms)	Ratio(HF/PLA)	PLA Loss %
						100.0						
	Carding	1										
	HF/PLA = 30/70	2										
		3										
		4					68.8					
	Needle Punching	1	Mat from Carding	0.0	0.0	68.8	68.8	0	0	0		
		2	Reverse	0.0	0.0	68.8	67.7	0.0	0.0	0.0		
		3	Fold/add PLA half	94.8	94.8	162.5	141.9	20.6	20.6	74.2	0.91	21.73
		4	Reverse	0.0	94.8	141.9	132.3	9.6	30.2	64.6	1.05	31.86
		5	Fold/add PLA half	94.8	189.6	227.1	219.0	8.1	38.3	151.3	0.45	20.20
		6	Go	0.0	189.6	219.0	215.9	3.1	41.4	148.2	0.46	21.84
		7	Go	0.0	189.6	215.9	213.5	2.4	43.8	145.8	0.46	23.10
		8	Go	0.0	189.6	213.5	211.8	1.7	45.5	144.1	0.47	24.00
		9	Go	0.0	189.6	211.8	210.0	1.8	47.3	142.3	0.48	24.95

A-2 TENSILE TESTING REPORTS

SAMPLE 1

Tuesday, April 12, 2016

INSTRON

Instron Applications Laboratory

ASTM D 638–08 Standard Test Method for Tensile Properties of Plastics

Conditioning procedure	
Preparation method	
Sample size	3
System of units	SI
Extensometer Class	Crosshead
Primary source	Extension
Dumbell Type	Type I
Control mode 1	Extension
Rate 1	2.00000 mm/min
Temperature (C)	23.0
Humidity (%)	50.0
Method revision date	11/2008

ASTM D 638-08: Stress-Strain Curve (Specimen 1 to 3)

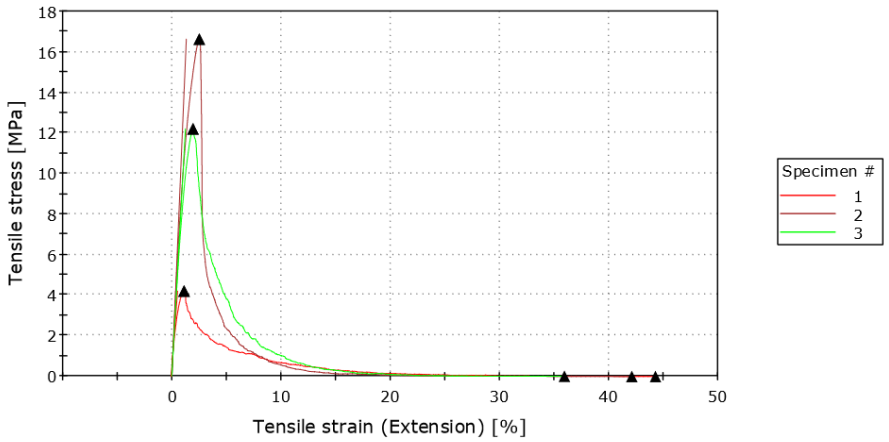

	Tensile Strength [MPa]	Tensile Strength at Yield [MPa]	% Elongation at Yield [%]	Tensile Strength at Break [MPa]	% Elongation at Break [%]	Modulus [MPa]	Modulus (Secant 1 %) [MPa]	Width [mm]	Thickness [mm]
1	4.22	4.22	1.10	0.0129	44.2	723	414	25.4	3.56
2	16.6	16.6	2.50	0.0121	42.1	1,260	995	25.4	3.78
3	12.2	12.2	1.92	0.0211	35.9	984	859	25.4	3.55
Mean	11.0	11.0	1.84	0.0154	40.7	990	756	25.4	3.63
S.D.	6.284	6.284	0.704	0.005	4.316	270	303.816	0.000	0.130

SAMPLE 2

Tuesday, April 12, 2016

INSTRON

Instron Applications Laboratory

ASTM D 638–08 Standard Test Method for Tensile Properties of Plastics

Conditioning procedure	
Preparation method	
Sample size	3
System of units	SI
Extensometer Class	Crosshead
Primary source	Extension
Dumbell Type	Type I
Control mode 1	Extension
Rate 1	2.00000 mm/min
Temperature (C)	23.0
Humidity (%)	50.0
Method revision date	11/2008

ASTM D 638-08: Stress-Strain Curve (Specimen 1 to 3)

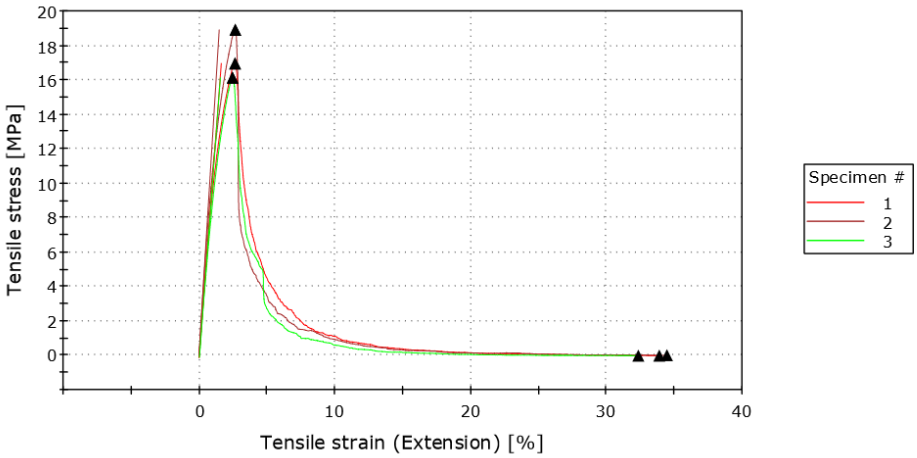

	Tensile Strength [MPa]	Tensile Strength at Yield [MPa]	% Elongation at Yield [%]	Tensile Strength at Break [MPa]	% Elongation at Break [%]	Modulus [MPa]	Modulus (Secant 1 %) [MPa]	Width [mm]	Thickness [mm]
1	17.0	17.0	2.66	0.0318	33.8	1,050	963	25.4	3.83
2	18.9	18.9	2.67	0.0509	34.4	1,280	1,080	25.4	3.81
3	16.1	16.1	2.46	0.0310	32.3	1,050	898	25.4	3.56
Mean	17.3	17.3	2.60	0.0379	33.5	1,130	980	25.4	3.73
S.D.	1.424	1.424	0.117	0.011	1.094	131	92.113	0.000	0.150

SAMPLE 3

Tuesday, April 12, 2016

INSTRON

Instron Applications Laboratory

ASTM D 638–08 Standard Test Method for Tensile Properties of Plastics

Conditioning procedure	
Preparation method	
Sample size	3
System of units	SI
Extensometer Class	Crosshead
Primary source	Extension
Dumbell Type	Type I
Control mode 1	Extension
Rate 1	2.00000 mm/min
Temperature (C)	23.0
Humidity (%)	50.0
Method revision date	11/2008

ASTM D 638-08: Stress-Strain Curve (Specimen 1 to 3)

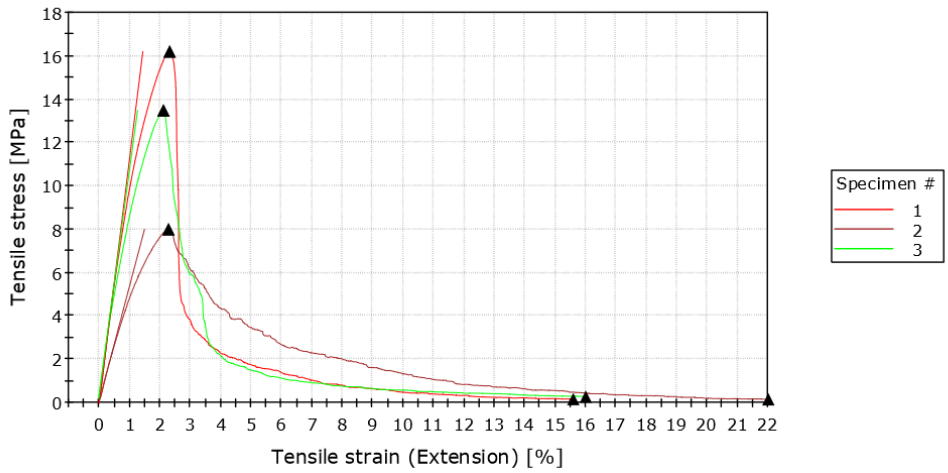

	Tensile Strength [MPa]	Tensile Strength at Yield [MPa]	% Elongation at Yield [%]	Tensile Strength at Break [MPa]	% Elongation at Break [%]	Modulus [MPa]	Modulus (Secant 1 %) [MPa]	Width [mm]	Thickness [mm]
1	16.2	16.2	2.33	0.197	15.6	1,120	976	25.4	3.52
2	8.01	8.01	2.29	0.183	22.0	531	480	25.4	3.49
3	13.5	13.5	2.12	0.315	16.0	1,030	852	25.4	3.66
Mean	12.6	12.6	2.25	0.232	17.9	894	769	25.4	3.56
S.D.	4.170	4.170	0.110	0.073	3.584	318	258.303	0.000	0.091

SAMPLE 4

Tuesday, April 12, 2016

INSTRON

Instron Applications Laboratory

ASTM D 638–08 Standard Test Method for Tensile Properties of Plastics

Conditioning procedure	
Preparation method	
Sample size	3
System of units	SI
Extensometer Class	Crosshead
Primary source	Extension
Dumbell Type	Type I
Control mode 1	Extension
Rate 1	2.00000 mm/min
Temperature (C)	23.0
Humidity (%)	50.0
Method revision date	11/2008

ASTM D 638-08: Stress-Strain Curve (Specimen 1 to 2)

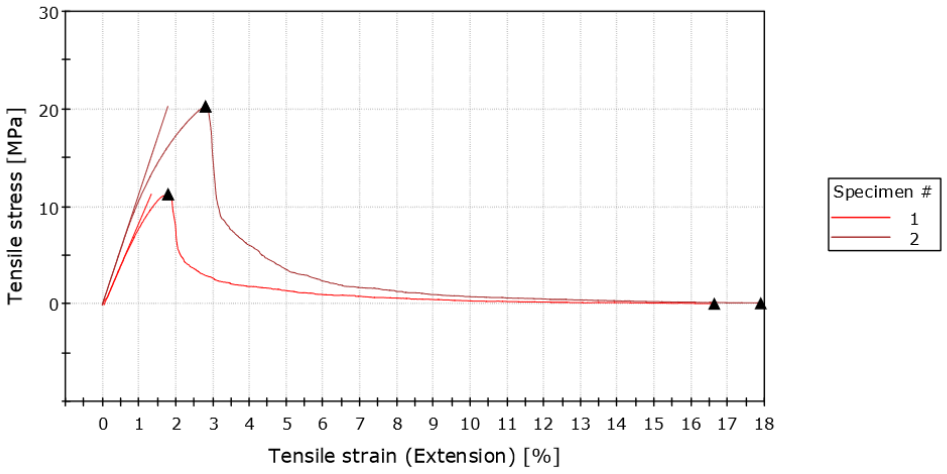

	Tensile Strength [MPa]	Tensile Strength at Yield [MPa]	% Elongation at Yield [%]	Tensile Strength at Break [MPa]	% Elongation at Break [%]	Modulus [MPa]	Modulus (Secant 1 %) [MPa]	Width [mm]	Thickness [mm]
1	11.3	11.3	1.79	0.107	16.6	880	777	25.4	3.41
2	20.3	20.3	2.80	0.171	17.9	1,130	1,070	25.4	3.40
Mean	15.8	15.8	2.30	0.139	17.2	1,010	921	25.4	3.40
S.D.	6.345	6.345	0.716	0.046	0.891	180	204.023	0.000	0.007

SAMPLE 5

Tuesday, April 12, 2016

INSTRON

Instron Applications Laboratory

ASTM D 638–08 Standard Test Method for Tensile Properties of Plastics

Conditioning procedure	
Preparation method	
Sample size	3
System of units	SI
Extensometer Class	Crosshead
Primary source	Extension
Dumbell Type	Type I
Control mode 1	Extension
Rate 1	2.00000 mm/min
Temperature (C)	23.0
Humidity (%)	50.0
Method revision date	11/2008

ASTM D 638-08: Stress-Strain Curve (Specimen 1 to 3)

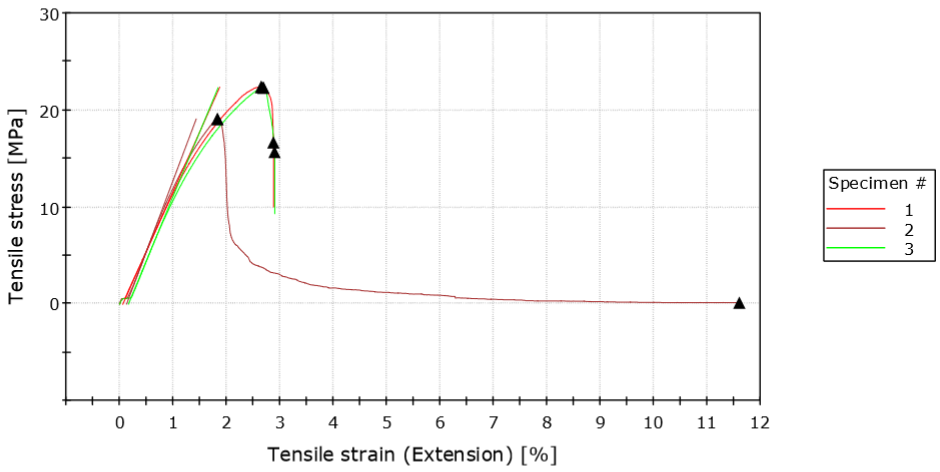

	Tensile Strength [MPa]	Tensile Strength at Yield [MPa]	% Elongation at Yield [%]	Tensile Strength at Break [MPa]	% Elongation at Break [%]	Modulus [MPa]	Modulus (Secant 1 %) [MPa]	Width [mm]	Thickness [mm]
1	22.4	22.4	2.66	16.7	2.88	1,230	1,140	25.4	3.51
2	19.1	19.1	1.83	0.158	11.6	1,460	1,190	25.4	3.47
3	22.3	22.3	2.69	15.7	2.90	1,330	1,060	25.4	3.47
Mean	21.3	21.3	2.39	10.8	5.79	1,340	1,130	25.4	3.48
S.D.	1.889	1.889	0.487	9.262	5.023	116	62.777	0.000	0.023

SAMPLE 6

Tuesday, April 12, 2016

INSTRON

Instron Applications Laboratory

ASTM D 638–08 Standard Test Method for Tensile Properties of Plastics

Conditioning procedure	
Preparation method	
Sample size	3
System of units	SI
Extensometer Class	Crosshead
Primary source	Extension
Dumbell Type	Type I
Control mode 1	Extension
Rate 1	2.00000 mm/min
Temperature (C)	23.0
Humidity (%)	50.0
Method revision date	11/2008

ASTM D 638-08: Stress-Strain Curve (Specimen 1 to 3)

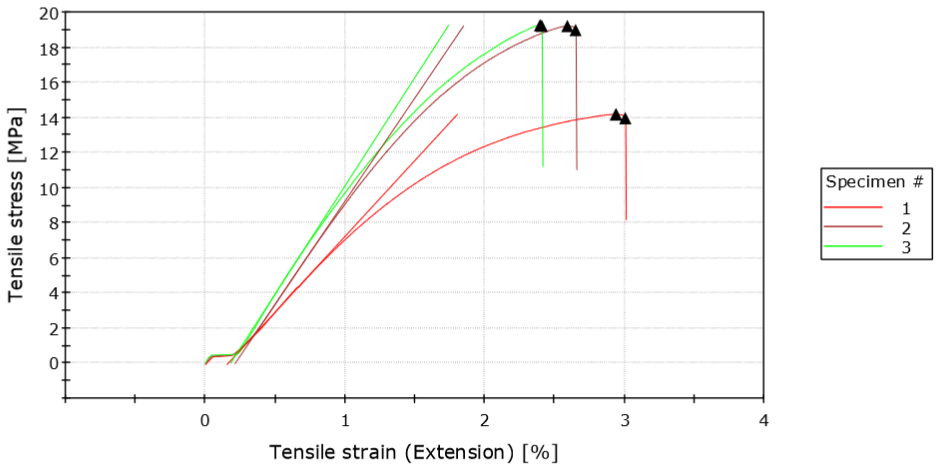

	Tensile Strength [MPa]	Tensile Strength at Yield [MPa]	% Elongation at Yield [%]	Tensile Strength at Break [MPa]	% Elongation at Break [%]	Modulus [MPa]	Modulus (Secant 1 %) [MPa]	Width [mm]	Thickness [mm]
1	14.2	14.2	2.94	14.0	3.00	863	706	25.4	4.85
2	19.2	-----	-----	19.0	2.65	1,170	908	25.4	4.11
3	19.2	-----	-----	19.2	2.41	1,230	973	25.4	4.10
Mean	17.5	14.2	2.94	17.4	2.69	1,090	863	25.4	4.35
S.D.	2.910	-----	-----	2.961	0.300	198	139.072	0.000	0.430

A-3 DYNAMIC MECHANICAL ANALYSIS GRAPHS

SAMPLE 1

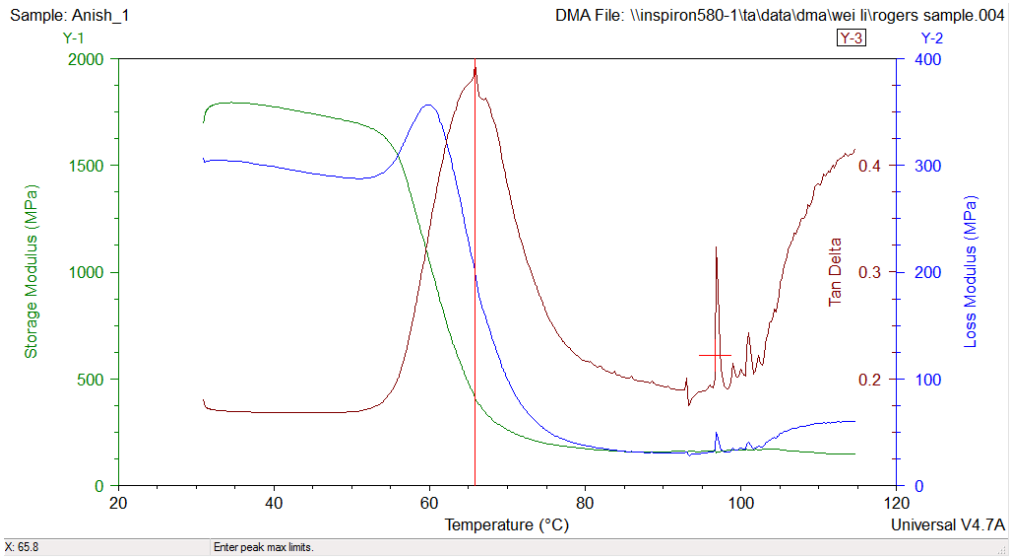

SAMPLE 2

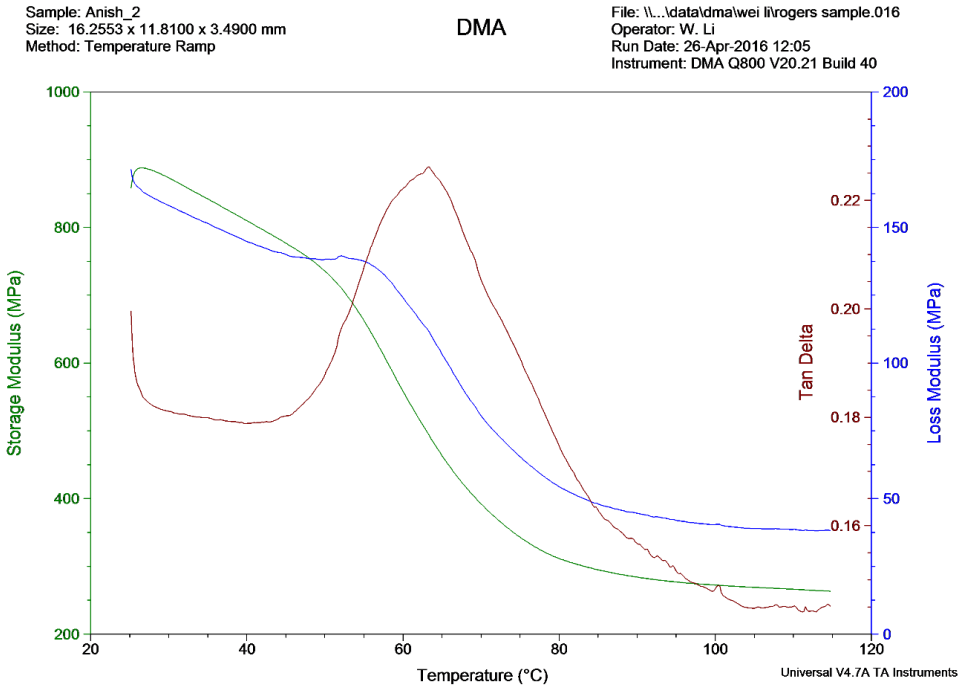

SAMPLE 3

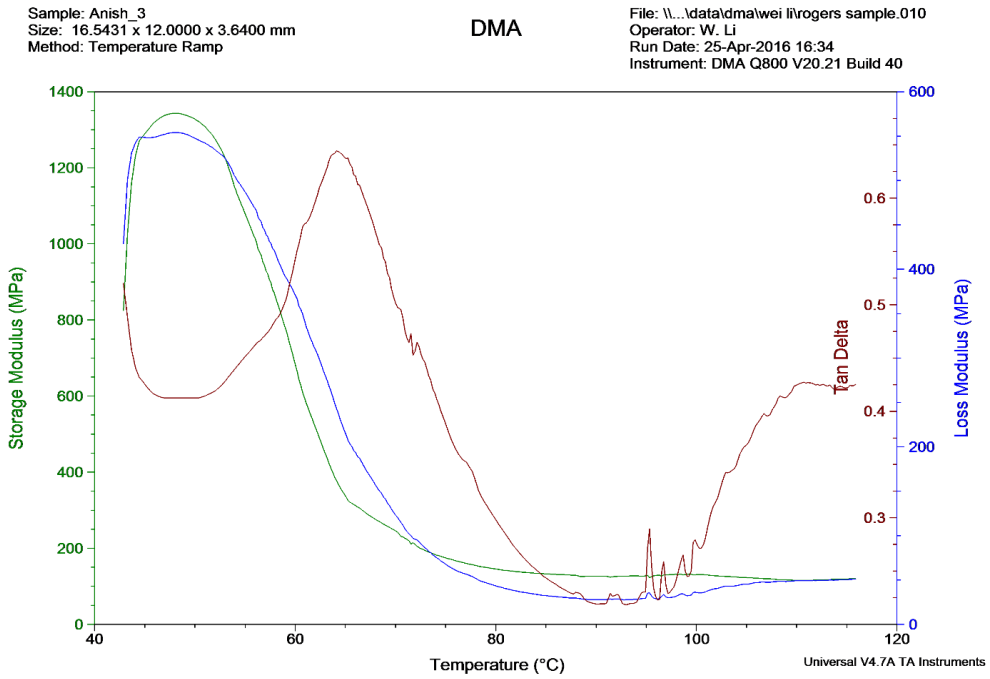

SAMPLE 4

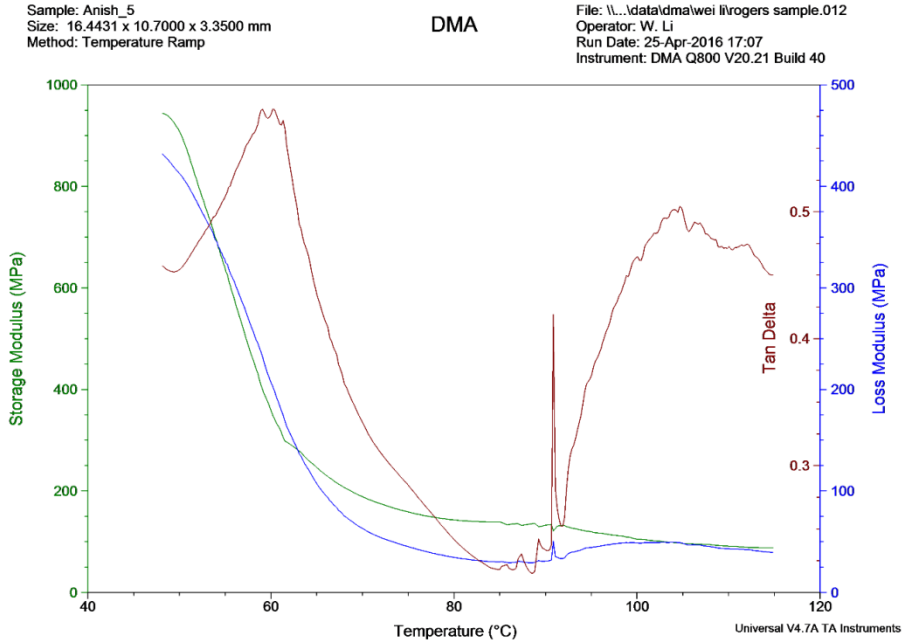

SAMPLE 5

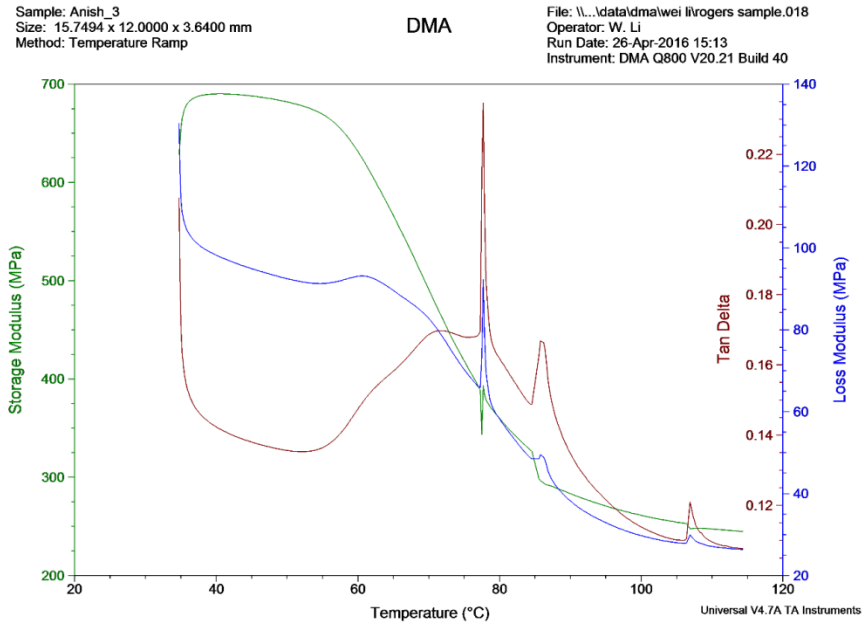

SAMPLE 6

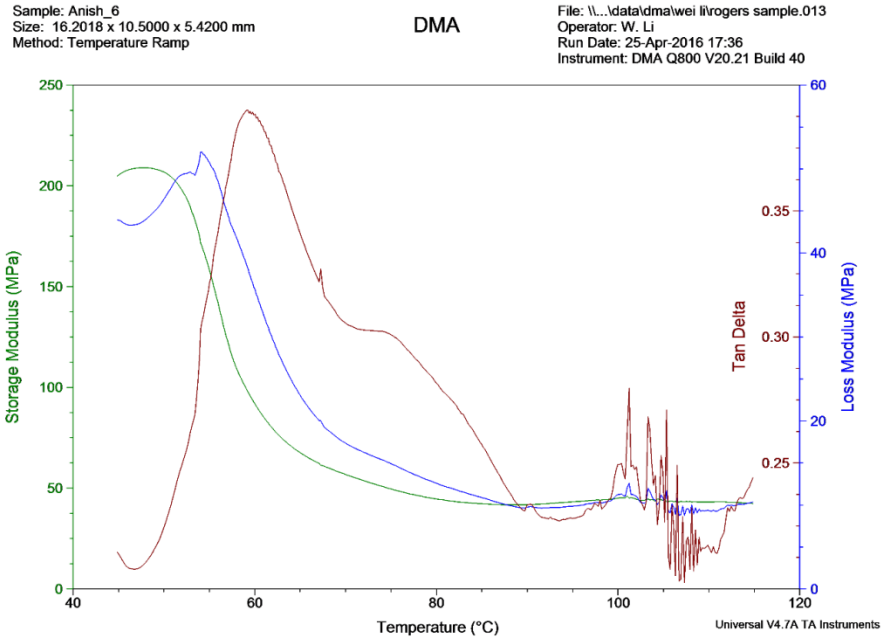

References

[1] S. Sakai, H. Yoshida, J. Hiratsuka, C. Vandecasteele, R. Kohlmeyer, V. Rotter, F. Passarini, A. Santini, M. Peeler and J. Li, "An international comparative study of end-of-life vehicle (ELV) recycling systems," *Journal of Material Cycles and Waste Management,* vol. 16, no. 1, pp. 1-20, 2014.

[2] P. Kemper and G. Hobi, "Copolyester Hot Melt Adhesives Combine with Nonwoven Fabrics," *Adhesives and Sealants Industry,* pp. 22-23, March 2003.

[3] "Eurostat," European Commission, 23 3 2016. [Online]. Available: http://appsso.eurostat.ec.europa.eu/nui/submitViewTableAction.do.

[4] R. Malkapuram, V. Kumar and S. Yuvraj, "Recent developments in natural fiber polypropylene composites," *Reinforced Plastics Composites,* vol. 28, pp. 1169-89, 2008.

[5] P. Wambua, J. Ivans and I. Verpoest, "Natura fibers: can they replace glass in fiber reinforced plastics," *Compos Sci Technol,* vol. 63, pp. 1259-64, 2003.

[6] S. Sapaun and N. Yusoff, "The Relationship Between Manufacturing and Design for Manufacturing in Product Development of Natural Fibre Composites," Springer International Publishing, Switzerland, 2015.

[7] "Fibersource," American Fiber Manufacturers Association, 1997. [Online]. Available: http://www.fibersource.com/f-tutor/techpag.htm.

[8] S. Kadolph and A. Langford, Textiles (9th edition), Pretence Hall, 2001.

[9] S. Warner, Fiber Science, New Jersey: Pretence Hall, 1995.

[10] C. Snyder, The extraordinary chemistry of ordinary things (3rd edition), New York: John Wiley, 1998.

[11] A. Frey-Wyssling, "The fine structure of cellulose microfibrils," *Science,* vol. 119, pp. 80-82, 1954.

[12] H. Chancy, "Cellulose Sources and Exploitation," in *Aspects of Cellulose Structure*, New York, Ellis Horwood Ltd., 1990.

[13] A. Bismarck, I. Aranberri-Askargorta, J. Springer, T. Lampke, B. Weilage, A. Stamboulis, I. Shenderovich and H. Limbach, "Surface characterization of flax, hemp and cellulose fibers:

surface properties and water uptake behaviour," *Poylm Compos,* vol. 23, pp. 872-894, 2002.

[14] A. Espert, F. Vilaplana and S. Karlsson, "Comparison of water absorption in natural cellulosic fibres from wood and one-year crops in polypropylene composites and its influence on their mechanical properties," *Compos Part A,* vol. 35, 2002.

[15] K. Pickering, G. Beckermann, S. Alam and N. Foreman, "Optimising industrial hemp fibre for composites," *Compos,* Vols. Part A-38, pp. 461-468, 2007.

[16] D. Dai and M. Fan, "Green modification of natural fibres with nanocellulose," *Rsc Adv,* vol. 3, pp. 4659-4665, 2013.

[17] A. Shahzad, "A Study in Physical and Mechanical Properties of Hemp Fibres," *Advanced in Material Science and Engineering,* p. 9, 2013.

[18] P. Yang and S. Kokot, "Thermal analysis of different cellulosic fabrics," *Journal of Applied Polymer Science,* vol. 60, pp. 1137-1146, 1996.

[19] F. Yao, Q. Wu, Y. Lei, W. Guo and Y. Xu, "Thermal decomposition kinetics of natural fibers: Activation energy with dynamic thermogravimetric analysis," *Polym Degrad Stab,* vol. 93, pp. 90-98, 2008.

[20] D. Saheb and P. Jog, "Natural fibre polymer composites: a review," *Advances in polymer technology,* vol. 18, no. 4, pp. 351-363, 199.

[21] B. Weilage, T. Lampke, G. Marx, K. Nestler and D. Starke, "Thermogravimetric and differential scanning calorimetric analysis of natural fibres and polypropylene," *Thermochimica Acta,* vol. 337, pp. 169-177, 1999.

[22] M. Sridhar, G. Basavarajjappa, S. Kasturi and N. Balsubramanian, "Thermal stability of jute fibers," *Indian journal of fiber and textile research,* vol. 7, pp. 87-91, 1982.

[23] C. Gonzalez and G. Myers, "Thermal degradation of wood fillers at the melt-processing temperatures of wood-plastic composites: effects on wood mechanical properties and production of volatiles," *Internation Journal of Polymerica Materials,* vol. 23, no. 1-2, pp. 67-85, 1993.

[24] S. Peter, Psychedelics Encyclopedia, Berkeley: Ronin Publishing, 1992.

[25] "FAOstat crop data," Food and Agriculture Organisation (FAO) of the United Nations, [Online]. Available: http://faostat.fao.org/. [Accessed 14 4 2016].

[26] D. Sedan, S. Pagnoux, A. Smith and T. Chotard, " Mechanical properties of hemp fibre reinforced cement: Influence of the fibre/matrix interaction," *J. Eur. Ceram. Soc,* vol. 23, p. 183, 2008.

[27] B. Prasad, M. Sain and D. Roy, "Properties of ball milled thermally treated hemp fibers in an inert atmosphere for potential composite reinforcement," *Journal of Material Science,* vol. 40, no. 16, pp. 4271-4278, 2005.

[28] "Mechanical properties of hemp fibers and hemp/pp composites: effects of chemical surface treatment," *Material Physics and Mechanics,* vol. 11, pp. 1-8, 2011.

[29] M. Fan, D. Dai and P. Collins, "Fabrication of nanocelluloses from hemp fibers and their application for the reinforcement of hemp fibers," *Industrial Crops and Products,* vol. 44, p. 192–199, 2013.

[30] R. Nelson, "Hemp Husbandry," *rexresearch,* 2000.

[31] R. Johnson, "Hemp as an Agricultural Commodity," *Congressional Research Service,* 2015.

[32] "FAOSTAT," FOOD AND AGRICULTURE ORGANIZATION OF THE UNITED NATIONS, 2015. [Online]. Available: http://faostat3.fao.org/browse/Q/QC/E.

[33] "Market Study - Bioplastics," Ceresana, 2016. [Online]. Available: http://www.ceresana.com/en/market-studies/plastics/bioplastics/.

[34] K. Jamshidi, S. Hyon and Y. Ikada, *Polmer,* vol. 29, pp. 2229-2234, 1998.

[35] M. Spinu, C. Jackson, M. Keating and K. Gardner, *Journal of Macromolecular Science—Pure and Applied Chemistry,* vol. A33, no. 10, pp. 1487-1530, 1996.

[36] C. Chen, J. Chueh, H. Tseng, H. Huang and S. Lee, "Preparation and characterization of biodegradable," *Biomaterials,* vol. 24, p. 1167–1173, 2003.

[37] W. Nuthonga, P. Uawongsuwan, W. Pivsa-Art and H. Hamada, "Impact Property of Flexible Epoxy Treated Natural Fiber Reinforced PLA," *Energy Procedia,* vol. 34, pp. 841-846, 2013.

[38] G. Perego, G. Cella and C. Bastioli, *Journal of Applied Polymer Science,* vol. 59, pp. 37-43, 1996.

[39] "Prospector," UL, [Online]. Available: http://plastics.ulprospector.com/generics/34/c/t/polylactic-acid-pla-properties-processing.

[40] J. Chen, A. Hao, H. Zhao, W. Jiang and L. Yuan, "Mechanical Properties of Kenaf/ Polypropylene Nonwoven Composites," *J Polym Environ.,* pp. 2-8, 2012.

[41] Y. Chen, O. Chiparus, L. Sun and I. Negulescu, "Natural Fibers for Automotive Nonwoven Composites," *Journal of Industrial Textiles,* vol. 35, no. 1, 2005.

[42] N. Martina, P. Daviesb and C. Baley, "Evaluation of the potential of three non-woven flax fiberreinforcements: Spunlaced, needlepunched and paper process mats," *Industrial Crops and Products,* vol. 83, pp. 194-205, 2016.

[43] T. Yuanjian and D. Isaac, "Impact and fatigue behaviour of hemp fibre composites," *Composites Science and Technology,* vol. 67, pp. 3300-3307, 2007.

[44] P. Uawongsuwan, W. Nuthong, W. Pivsa-Arta and H. Hamada, "Impact Property of Flexible Epoxy Treated Natural Fiber Reinforced PLA Composites," *Energy Procedia,* vol. 34, pp. 839-847, 2013.

[45] M. Jawaid, H. Abdul Khalil, A. Bhat and A. Baker, "IMPACT PROPERTIES OF NATURAL FIBER HYBRID REINFORCED EPOXY COMPOSITES," *Advanced Materials Research,* Vols. 264-265, pp. 690-692, 2011.

[46] M. Zampaloni, F. Pourboghrat, S. Yankovich, B. Rodgers, J. Moorea, L. Drzal, A. Mohanty and M. Misra, "Kenaf natural fiber reinforced polypropylene composites: A discussion on manufacturing problems and solutions," *Composites Part A: Applied Science and Manufacturing,* vol. 38, no. 6, p. 1569–1580, 2007.

[47] K. Pickering, M. Efendy and T. Le, "A review of recent developments in natural fibre composites," *Composites: Part A,* vol. 83, p. 98–112, 2016.

[48] A. Haoa, J. Chen and H. Zhaob, "Kenaf/polypropylene nonwoven composites: The influence of manufacturing conditions on mechanical, thermal, and acoustical performance," *Composites,* vol. Part B, no. 54, pp. 44-51, 2013.

[49] T. Behzad and M. Sain, "Measurement and Prediction of Thermal Conductivity forHemp Fiber Reinforced Composites," *POLYMER ENGINEERING AND SCIENCE,* 2007.

[50] R. Osugi, H. Takagi, K. Liu and Y. Gennai , "THERMAL CONDUCTIVITY BEHAVIOR OF NATURAL," in *Asian Pacific Conference for Materials and Mechanics*, Yokohoma, 2009.

[51] "The Engineering Toolbox," [Online]. Available: http://www.engineeringtoolbox.com/thermal-conductivity-plastics-d_1786.html. [Accessed 2016].

[52] J. Chen, D. Muller, C. Konig, K. Neiben and J. Mussig, "Spunlaced flax/polypropylene non-woven as automotive interior - Acoustical and fogging performance," *Journal of Biobased material and Bioenergy,* vol. 4, no. 4, pp. 330-337, 2010.

[53] C. Koenig and D. Mueller, "Acoustical properties of reinforced composite materials basing on natural fibers.," *Acoustics,* 2008.

[54] N. Yilmaz and Powell, " The Technology of Terry Towel production," *Journal of Textile and Apparel, Technology and Management,* vol. 4, 2005.

[55] G. Beckermann and K. Pickering, "Engineering and evaluation of hemp fibre reinforced polypropylene composites: fibre treatment and matrix modification," *Composites A,* vol. 39, no. 6, pp. 979-988, 2008.

[56] J. Lisperguer, P. Perez and S. Urizar, "STRUCTURE AND THERMAL PROPERTIES OF LIGNINS: CHARACTERIZATION BY INFRARED SPECTROSCOPY AND DIFFERENTIAL SCANNING CALORIMETRY," *Journal of the Chilean Chemical Society,* vol. 54, no. 4, pp. 460-463, 2009.